The occurrence and hazards of great subduction zone earthquakes

Erin A. Wirth[1,6]✉, *Valerie J. Sahakian*[2,6]✉, *Laura M. Wallace*[3,4] *and Daniel Melnick*[5]

Abstract | Subduction zone earthquakes result in some of the most devastating natural hazards on Earth. Knowledge of where great (moment magnitude **M** ≥ 8) subduction zone earthquakes can occur and how they rupture is critical to constraining future seismic and tsunami hazards. Since the occurrence of well-instrumented great earthquakes, such as the 2004 **M**9.1 Sumatra–Andaman and 2011 **M**9.1 Tohoku earthquakes, the hypotheses that plate age and convergence rate influence the ability of subduction zones to host large earthquakes have been dispelled. In this Review, we highlight how certain subduction zone properties might influence the location and characteristics of great earthquake rupture and impact seismic and tsunami hazard. The rupture characteristics of great earthquakes that most heavily impact earthquake hazards include the rupture extent (seaward and landward), location of strong motion-generating areas and earthquake recurrence. By contrast, large slip or displacement at the seafloor is one of the major controls of tsunami hazard. Future improvements in addressing hazards posed by subduction zones depend heavily on sustained geophysical monitoring in subduction zone systems (both onshore and offshore), expanded development of palaeoseismic data sets and improved integration of observations and models across disciplines and timescales.

Ground motions
Movements of the Earth's surface due to seismic waves from earthquakes or explosions.

[1]*US Geological Survey, Earthquake Science Center, Seattle, WA, USA.*

[2]*Department of Earth Sciences, University of Oregon, Eugene, OR, USA.*

[3]*GNS Science, Lower Hutt, New Zealand.*

[4]*University of Texas, Institute for Geophysics, Austin, TX, USA.*

[5]*Instituto de Ciencias de la Tierra, Universidad Austral de Chile, Valdivia, Chile.*

[6]*These authors contributed equally: Erin A. Wirth, Valerie J. Sahakian.*

✉*e-mail: ewirth@usgs.gov; vjs@uoregon.edu*

https://doi.org/10.1038/s43017-021-00245-w

Subduction zone earthquakes and their cascading consequences result in some of the most devastating natural hazards on Earth. In particular, earthquakes larger than a moment magnitude, **M** (BOX 1), of 8.0 (termed 'great earthquakes') produce such a vast energy release that they can cause severe damage in areas several hundreds of kilometres across. For example, the catastrophic earthquakes in Japan (2011) and Indonesia (2004) collectively caused more than 250,000 fatalities and more than US$210 billion in economic damage, combined[1–3]. Mitigating this risk in the future requires improved infrastructure and emergency response, which in turn necessitates a better understanding of the geohazards posed by great earthquakes.

Great earthquakes most commonly occur at convergent plate boundaries, where two tectonic plates converge and one is subducted beneath the other along a megathrust fault boundary. During the interseismic period between earthquakes the tectonic plates can become frictionally locked together, resulting in an accumulation of stress owing to tectonic loading[4]. Over time, sufficient stress accumulates along the subduction interface, until it eventually exceeds the strength of the fault and is released as seismic energy during an earthquake.

Numerous hazards are associated with the remarkable size of **M** ≥ 8 events. Great megathrust earthquakes can produce violent ground motions and cascading hazards such as landslides, coastal land-level change and liquefaction, as witnessed in the 2010 **M**8.8 Maule and 2011 **M**9.1 Tohoku earthquakes[5–7]. Tsunamis are typically generated by earthquakes that rupture the shallow, offshore portion of the megathrust fault. Greater displacement of the seafloor contributes to larger tsunamis resulting in considerable loss of life and infrastructure damage, such as the more than 200,000 fatalities during the 2004 **M**9.1 Sumatra–Andaman earthquake and tsunami[8,9].

Knowledge of subduction zone earthquake processes is currently observation-limited. Although most global subduction zones host large earthquakes, the largest events are fortunately rare on human timescales. However, their rarity limits statistically significant observations of great earthquake occurrence and associated hazards. Despite these observational limitations, there have been substantial advances in understanding great megathrust earthquakes since the early twenty-first century, owing to increases in data density and quality. Notably, the 2011 **M**9.1 Tohoku, Japan event occurred in a densely instrumented region and was exceptionally well recorded both onshore and offshore in the near field (<500 km). These observations improved our ability to image and understand the potential for large (>60 m) amounts of shallow slip, and its relationship to catastrophic tsunamis[10]. The 2004 **M**9.1 Sumatra–Andaman earthquake was not as well-instrumented locally, yet is

Key points

- Numerous hazards are associated with the remarkable size of moment magnitude **M** ≥ 8 megathrust earthquakes, such as landslides, coastal land-level change, liquefaction and tsunamis.
- Understanding the likelihood of subduction zone earthquake occurrence and their rupture physics is crucial to creating probabilistic hazard assessments and to mitigating future risks.
- Seismic and geodetic instrumentation combined with advanced modelling techniques have brought about notable advances in understanding great subduction zone earthquakes, unveiling more about the source processes of great earthquakes, and the structure and state of stress in subduction zones.
- Improved data sets and additional observations of great earthquakes have refocused attention on a more diverse range of subduction zone properties and processes required for great earthquakes to occur, but still lack the statistical significance required to make broad claims about where and when great subduction zone earthquakes are likely to occur.
- Great earthquakes occur infrequently; improving characterizations of great megathrust earthquake occurrence for probabilistic seismic hazard assessments will require additional geologic and geophysical observations and constraints, as well as numerical models.

another example of a big event with modern recordings. It ruptured an unprecedented length (1,300 km) of the megathrust fault zone.

The development of seafloor geodetic methods and the integration of geological, seismological and geodetic observations have brought a wave of new inferences regarding large earthquake source processes. For example, integration of studies before and after the 2011 Tohoku earthquake elucidated relationships between megathrust frictional properties, seismicity and slip[11]. As a result of such synergistic works, the spectrum of deformation styles occurring throughout the seismic cycle has been further illuminated. Together, these advances have underscored the complexity of properties along the plate interface and their relationship to megathrust earthquake behaviour.

In this Review, we discuss the conditions required to generate great megathrust earthquakes and the characteristics of subduction systems that have previously hosted these earthquakes. In particular, we focus on advances since the 2010 **M**8.8 Maule, Chile and 2011 **M**9.1 Tohoku, Japan earthquakes. We also discuss the earthquake rupture parameters (for example, downdip extent, rupture speed, strong motion-generating areas, tsunami generation) that most heavily impact hazard, and how they might be related to subduction system characteristics. Finally, we highlight some of the key uncertainties currently limiting probabilistic seismic and tsunami hazard models in subduction zones and suggest priorities for future research.

Seismic cycle
A repetitive process during which tectonic stress on a fault builds up over time and then is rapidly released during (coseismic) and after (post-seismic) an earthquake.

Partially locked
When a fault is slipping at some rate between zero and the long-term relative plate motion rate.

Fully locked
When a fault releases zero slip during the interseismic period.

Quasi-periodic behaviour
Earthquake recurrence that exhibits simple, nearly periodic recurrence intervals between earthquakes.

Box 1 | **Seismic moment**

Earthquake moment magnitude **M** is a logarithmic representation of an earthquake's seismic moment, or total energy release of an earthquake. The seismic moment of an earthquake (M_0) is defined as $M_0 = \mu \times A \times D$. Assuming that the average shear modulus (μ) is relatively similar across global subduction zones, seismic moment is primarily a function of rupture area (A), controlled by fault width and length, and the amount of slip (D). Note that some scaling relationships suggest the fault width saturates for very large-magnitude events[190,191].

The occurrence of great earthquakes

Based on both short instrumental and longer geologic records, great earthquakes (**M** ≥ 8.0) seem to be observed with regularity only at certain subduction zones, such as in Japan, Alaska, Cascadia, South America and Indonesia (FIG. 1). Since 1960, only four giant earthquakes (**M** ≥ 9.0) have occurred globally[12], posing scientific challenges in relating their occurrence and rupture characteristics to subduction zone parameters. These great and giant earthquakes often generate sizable tsunamis, with the maximum tsunami water height dictated by the extent to which the seafloor deforms, the local bathymetry and the presence of submarine ground failures. In the case of some giant earthquakes, maximum tsunami wave heights have exceeded 30 m (REF.[13]).

The seismic cycle

During the time between large subduction thrust earthquakes, the subducting and overriding tectonic plates can be partially locked or fully locked together, accumulating stresses that will ultimately be released in future seismic events. Geodetic techniques can be used to measure the accumulation of elastic strain in Earth's crust, and to resolve the location and extent to which plates are locked together and accumulating stress[14]. In some large subduction earthquakes, the ruptured portions of the megathrust generally coincided with regions where the interface was locked prior to the earthquake[15–18], suggesting that the distribution of interseismic locking might provide a useful guide to anticipate the locations of future ruptures[15]. However, geodetic measurements of contemporary interseismic locking largely only date back to approximately the 1990s, and therefore do not allow assessment of possible spatio-temporal variability over multiple seismic cycles.

Although the relationship between locations of interseismic locking and slip during great earthquakes is generally accurate for some megathrust earthquakes, this conceptualized model does not capture the complex spatio-temporal patterns observed in great earthquake behaviour over multiple seismic cycles. Global instrumental and geologic observations suggest that some subduction zones exhibit a seismic cycle with simple quasi-periodic behaviour[19,20]. Others demonstrate substantial variability in earthquake magnitude, rupture area and recurrence interval between events in the same region[21,22].

Megathrust sections that are known or thought to have previously produced great earthquakes, but which have not done so for a considerable period, are also observed. These 'seismic gaps' might delineate portions of the megathrust that are likely to rupture as great earthquakes in the future[12,23]. As an example, the 2010 **M**8.8 Maule, Chile event occurred in a known seismic gap, where a similar earthquake last occurred in 1835 (FIG. 1). The Maule event ruptured a seismic gap between the 1960 **M**9.5 Valdivia earthquake to the south and a 1928 **M**8.0 earthquake to the north, while also partially or fully overlapping with the rupture areas of both the 1960 and 1928 events, respectively[24–26].

Seismogenic zone
The region of the megathrust fault capable of generating earthquakes.

Velocity-weakening
When a fault exhibits a decrease in frictional strength with increased sliding velocity, promoting earthquake rupture. Velocity weakening friction is a prerequisite for the nucleation of unstable (seismic) slip.

The seismic gap model is, however, sometimes contested on the basis of insufficient observations for statistically significant tests[27,28]. As with many of the descriptive models reviewed here, exceptions might be present, and fully utilizing seismic gap theory requires knowledge of historical ruptures and spatio-temporal variability in locking[29], which is often not available.

Depth-varying frictional properties

In addition to exhibiting spatio-temporal variability, great earthquakes demonstrate a large range of behaviours in their rupture physics. Great earthquakes nucleate within the seismogenic zone, the portion of the megathrust where fault rocks exhibit velocity-weakening behaviour, thus promoting earthquake nucleation and rupture[30,31]. Conditionally stable regions can exist both updip and downdip of the seismogenic zone, as well as within distributed patches throughout the seismogenic zone itself, and are typically the site of slow slip events (SSEs)[32]. Generally, such conditionally stable regions straddle the frictional transition from velocity-weakening to velocity-strengthening. However, dynamic rupture can induce stress changes that allow slip to occur in these conditionally stable regions during an earthquake[33]. As temperatures increase with

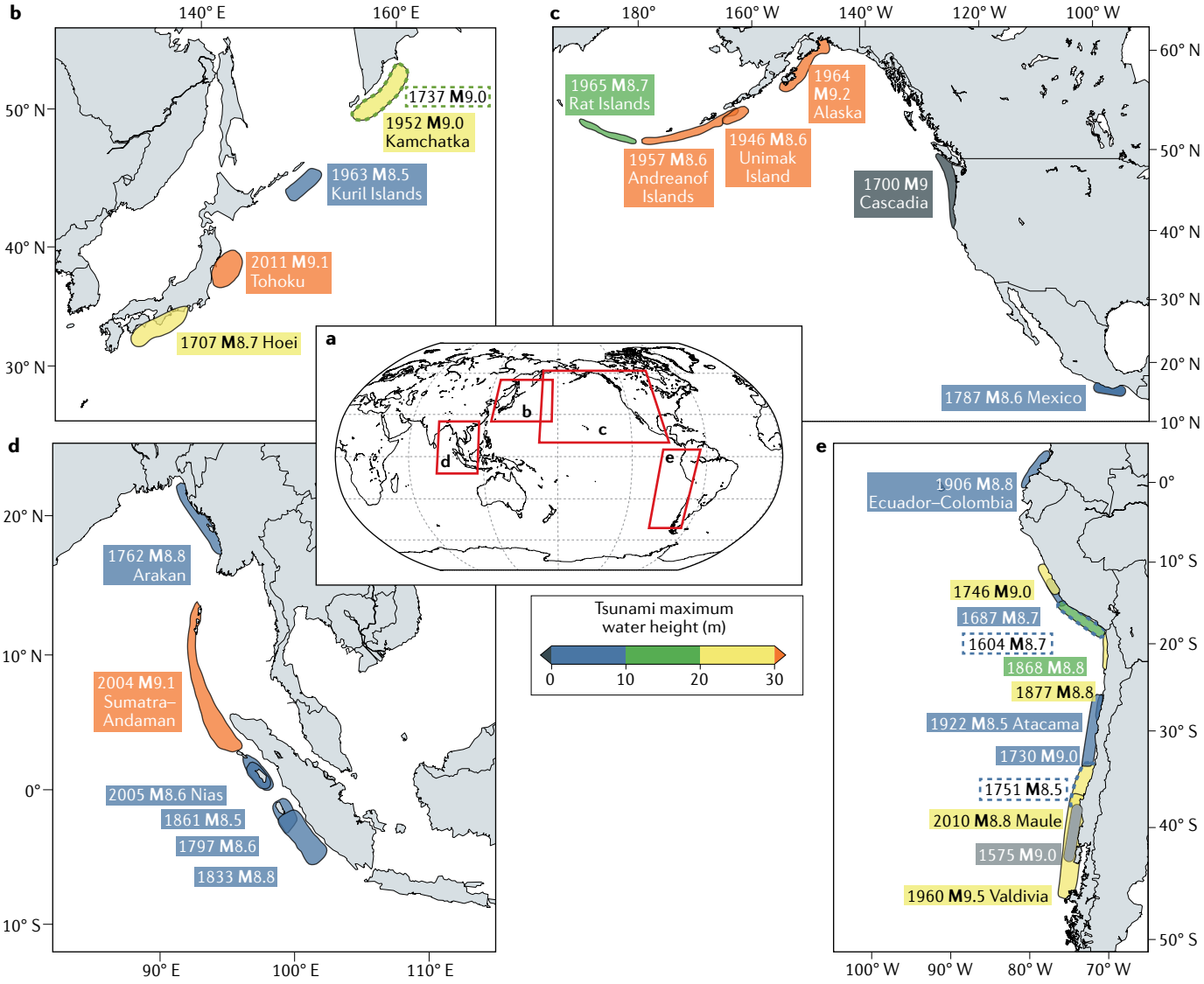

Fig. 1 | **Map of recorded and historical M ≥ 8.5 megathrust earthquakes.** **a** | Global map showing locations of panels **b**–**e**. **b** | Japan–Kuril–Kamchatka subduction margin. **c** | Aleutian–Cascadia and Mexican subduction zones. **d** | Andaman–Sumatra–Java margin. **e** | South American margin. Historical earthquakes (pre 1906) were required to be robustly constrained by published historical and/or geological evidence. Associated rupture areas and moment magnitudes (**M**) should be considered approximate. Historical earthquakes with rupture areas similar to instrumentally well-constrained earthquakes are shown as dashed outlines. Earthquakes are colour-coded based on the maximum water height of their associated tsunami from the NOAA Global Historical Tsunami Database (https://www.ngdc.noaa.gov/hazard/tsu_db.shtml). Tsunami heights are influenced by the earthquake source, and also by local bathymetry and ground failures. Earthquakes that generated local tsunamis of unknown height are shaded grey. Rupture areas are from REFS[96,174–182] and references therein. Additional information regarding these earthquakes is provided in Supplementary Note 1. This representation of recorded and historical ruptures illustrates the locations where great earthquakes are either absent or there is a lack of sufficient evidence for past ruptures, and underscores the prolificness of other subduction zones in generating great earthquakes.

Conditionally stable
When a fault exhibits frictional stability under static loading conditions but could become unstable (seismic) under sufficiently strong dynamic loading.

Slow slip events
(SSEs). Episodic aseismic slip events lasting days to years that result in a few to tens of centimetres of slip along a fault.

depth along the megathrust, ductile behaviour eventually dominates the system, leading to steady, aseismic slip (creep) below the seismogenic and slow slip zones[32]. The location of the seismogenic zone is governed, in part, by frictional and thermal properties, so each subduction zone's seismogenic region is expected to vary based on its geometry, age, kinematics and composition.

Depth-varying slip behaviour

The megathrust has previously been conceptually divided into depth-varying slip domains that broadly explain earthquake and seismogenic zone characteristics[32,34,35].

The shallowest, updip domain is thought to extend from approximately the trench to <15 km depth and is capable of either aseismic or coseismic deformation (FIG. 2). This updip region is characterized by weak, low-rigidity materials and fluid-rich rocks with primarily velocity-strengthening and/or conditionally stable frictional properties[36,37], and is rarely the site of great earthquake nucleation. Large coseismic slip in the updip domain is usually (but not always) a consequence of energetic events originating in the seismogenic zone below. The physical properties of updip regions result in inefficient seismic radiation that produces low levels of ground shaking onshore, such as during the 2010 **M**7.8 Mentawai earthquake[38,39] (FIG. 2). When coseismic slip in this updip region vertically displaces the seafloor, it can perturb the overriding water column and lead to tsunami generation. Tsunami earthquakes are earthquakes occurring in the updip region that produce tsunamis substantially larger than expected based on their magnitude[40,41]; for example,

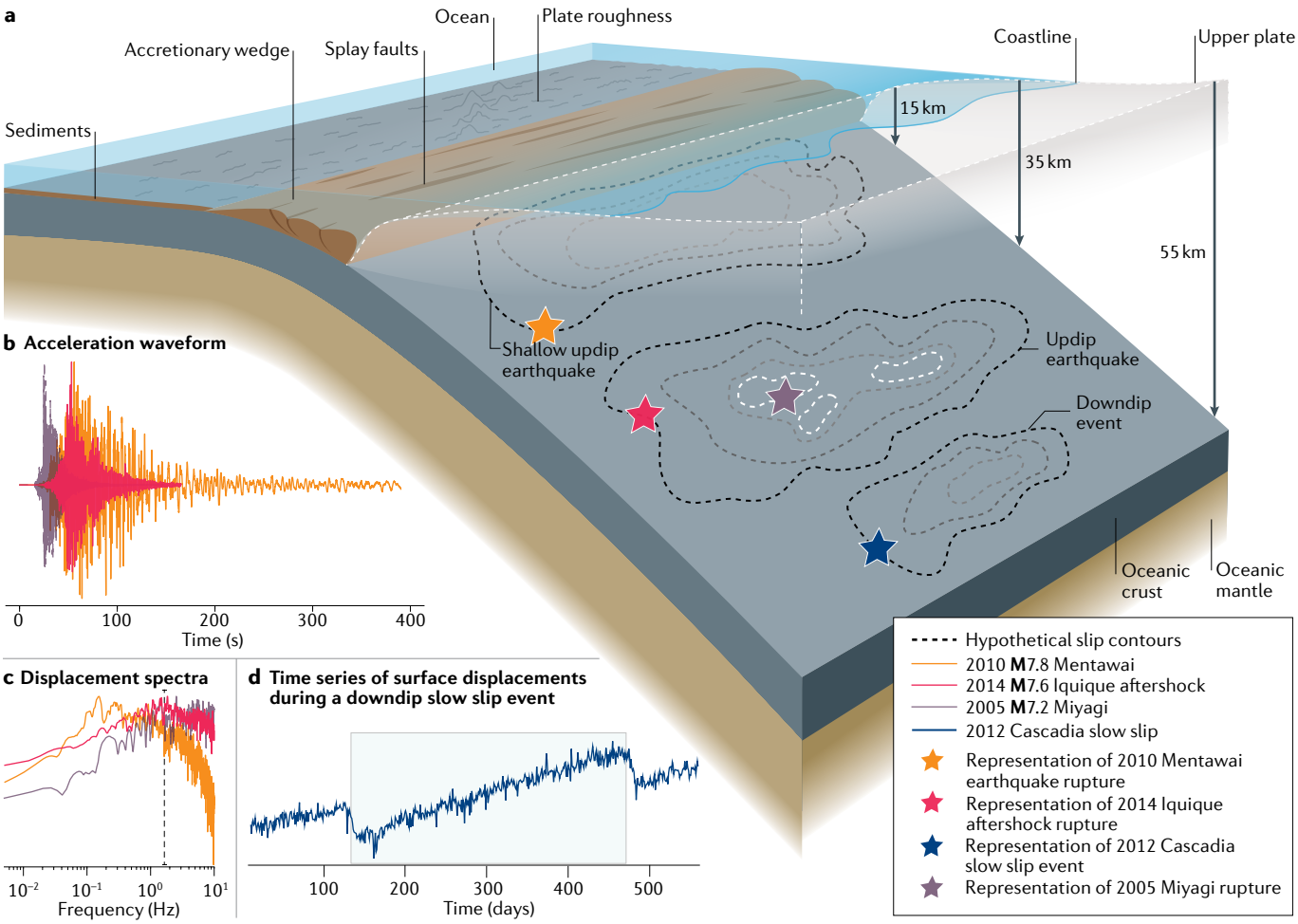

Fig. 2 | **Subduction zone structures, behaviour and their relationship to hazard. a** | Geometry, roughness and sediment thickness on the incoming plate can impact earthquake occurrence. Rupture of the shallowest (less than ~15 km), updip portion of the megathrust and splay faults is important for tsunamigenesis. Events occurring solely in this region (tsunami earthquakes) can rupture with high amounts of slip, yet are depleted in high-frequency energy (Mentawai event). Seismogenic zone events at intermediate depths (~15–35 km) tend to produce earthquakes with higher-frequency energy (for example, the Iquique aftershock), with deeper events and asperities producing higher stress drops and high-frequency radiation (for example, the Miyagi event). These relatively higher frequencies can be seen in example normalized event waveforms and spectra in panels **b** and **c**. Seismogenic zone event acceleration waveforms (panel **b**) and spectra (panel **c**) from the 2010 moment magnitude **M**7.8 Mentawai (yellow), 2014 **M**7.6 Iquique aftershock (pink) and 2005 **M**7.2 Miyagi (purple) events. **d** | Displacement waveform from a 2012 downdip slow slip event (SSE) in Cascadia (blue). Vertical dashed line on the spectra in panel **c** indicates the location where the Iquique aftershock becomes depleted in higher-frequency energy, whereas the Miyagi event remains enriched. At a range of depths, subduction zones can exhibit transitional domains that host episodic SSEs. Waveforms and their acceleration spectra are normalized from stations at approximately the same hypocentral distance and, except for the SSE, are from REF.[39]. Shaking and seismic hazards are intimately linked to subduction zone architecture and slip behaviour.

Velocity-strengthening
When a fault exhibits frictional strength that increases with sliding, promoting aseismic slip or creep.

Tsunami earthquakes
Slow earthquakes that rupture the shallow (typically <15 km) megathrust and produce anomalously large tsunamis for their magnitude. Tsunami earthquakes also exhibit a depletion of high-frequency seismic energy.

Afterslip
Aseismic slip that typically occurs on a fault following seismic rupture and can last for months to years and is often associated spatio-temporally with aftershocks.

Seismic hazard
In general, any physical phenomenon caused by an earthquake that could produce adverse effects (ground shaking, landslides, liquefaction, land-level change and so on). More specifically, seismic hazard refers to the likelihood of exceeding a threshold level of shaking or ground motion in a particular region and time frame.

an earthquake of ~**M**7.8 is expected to produce ~2–5 m run-up, but the 2010 **M**7.8 Mentawai tsunami earthquake produced up to 16 m of run-up[41].

The main portion of the seismogenic zone (typically between ~15 km and 35 km depths) is generally thought to be characterized by broad, frictionally unstable regions (asperities) that are capable of nucleating earthquakes and producing large coseismic displacements[39,42]. At greater depths (~35–55 km), these velocity-weakening patches become smaller and tend to produce only moderate amounts of coseismic slip. They are, however, capable of radiating substantial amounts of high-frequency energy compared with the shallower portion of the seismogenic zone, such as observed during the 2005 **M**7.2 Miyagi earthquake[43–46] (FIG. 2).

At depths above and below the seismogenic zone, many subduction systems exhibit a transitional domain that hosts SSEs[47,48]. SSEs are typically detected using a range of geodetic methods and are often linked to seismic phenomena including tectonic tremor and low-frequency earthquakes[49–51]. SSEs have been observed at virtually all subduction zones that are well instrumented with continuously operating geodetic networks, suggesting that they are a phenomenon common to most, if not all, subduction zones. Episodic SSEs are thought to occur on faults in conditionally stable regions that occupy the transition between seismic and aseismic behaviour. Thus, these SSEs often occur adjacent to the locked seismogenic zone, potentially providing further insight into which portions of the plate boundary might be prone to rupture in large earthquakes (FIG. 2).

SSEs have been observed at a range of depths on subduction megathrusts, including deep (>25 km depth)[49,51–53] and shallow events, some of which have propagated all the way to the trench (<15 km)[54–56]. In a few cases, SSEs have been observed in the lead up to great subduction zone earthquakes, potentially playing a role in triggering these events (2011 **M**9.1 Tohoku[57]; 2014 **M**8.2 Iquique[58]). Although distinct from episodic SSEs, transient aseismic slip is also typically observed for years to decades following great megathrust earthquakes (referred to as afterslip)[59].

Overall, the characteristics of earthquake rupture exert strong controls on the amplitude, frequency and duration of ground motions, which, together with earthquake magnitude and recurrence intervals, control seismic hazard. Seismic imaging, modelling, laboratory and observational studies have made strides in understanding the physical processes that might play a role in defining the observed spatio-temporal patterns and elucidating the possible relationships between subduction zone structure and earthquake rupture characteristics. In the ensuing sections, the most promising efforts to ascribe specific subduction zone parameters to megathrust earthquake occurrence are discussed. However, there are likely complex feedbacks between these parameters that are not yet fully understood.

Influence of subduction zone properties

Developing a physical model for the relationship between subduction zone characteristics and earthquake magnitude and location has been of interest since the broader acceptance of plate tectonics. Such a model would be key in developing improved seismic hazard estimates in subduction zone settings. Here, we discuss some of the subduction characteristics that seem most likely to allow an initiated earthquake to propagate across an extensive area and produce large amounts of slip, resulting in a large earthquake.

Earthquake size

There is a distinction between the conditions necessary to promote the nucleation of a megathrust earthquake versus those that are required for it to grow into a truly great earthquake (**M** ≥ 8.0). Earthquakes initiate in regions where the accumulated stress exceeds the local fault strength. In some cases, the nucleation of great earthquakes has been attributed to concentrated stresses owing to adjacent locked and creeping sections on the fault[60] or in areas where there are perturbations to the regional stress field because of rough subducting topography (for example, subducting seamounts)[61,62]. However, once nucleated, subduction zones with characteristics that promote rupture over a large spatial extent and/or host large seismic slip are more likely to produce the largest megathrust earthquakes, and are directly related to the parameters that define seismic moment and magnitude (BOX 1). In the subsequent sections, the parameters that seem demonstrably favourable for promoting rupture propagation over a large region and large coseismic slip in subduction zones are considered.

Subduction parameters

Numerous attempts have been made to draw correlations between a range of subduction parameters and earthquake occurrence, with mixed success (FIG. 3). Early work hypothesized that the plate age and convergence rate dictated the maximum magnitude of subduction zone earthquakes, with young, more rapidly subducting plates resulting in the largest events because of increased coupling[63] (FIG. 3a,b). However, this view has been overturned by subsequent large events, including the 2004 **M**9.1 Sumatra–Andaman and 2011 **M**9.1 Tohoku earthquakes, which occurred in subduction systems with relatively slow convergence (the Andaman trench) or old, cold subducting oceanic lithosphere (Tohoku). For **M** ≥ 8.5 earthquakes, the plate age and convergence rate do not appear to correlate with earthquake magnitude with meaningful statistical significance (FIG. 3).

Numerical models show a negligible effect of the convergence rate on the generation of great earthquakes and it has been suggested that subduction zones with fast convergence rates might simply experience more frequent earthquakes, thus increasing the chance of observing a large megathrust event in the historical record[64]. However, the convergence rate might influence the width of the seismogenic zone to some degree, as slabs subducting at a faster rate will stay colder to deeper depths, thus elongating the along-dip length of the seismogenic zone[65]. Subsequent studies have suggested that stronger correlations exist between the maximum magnitude of megathrust earthquakes and parameters related to subduction zone geometry, subducting sediment thickness, incoming plate roughness

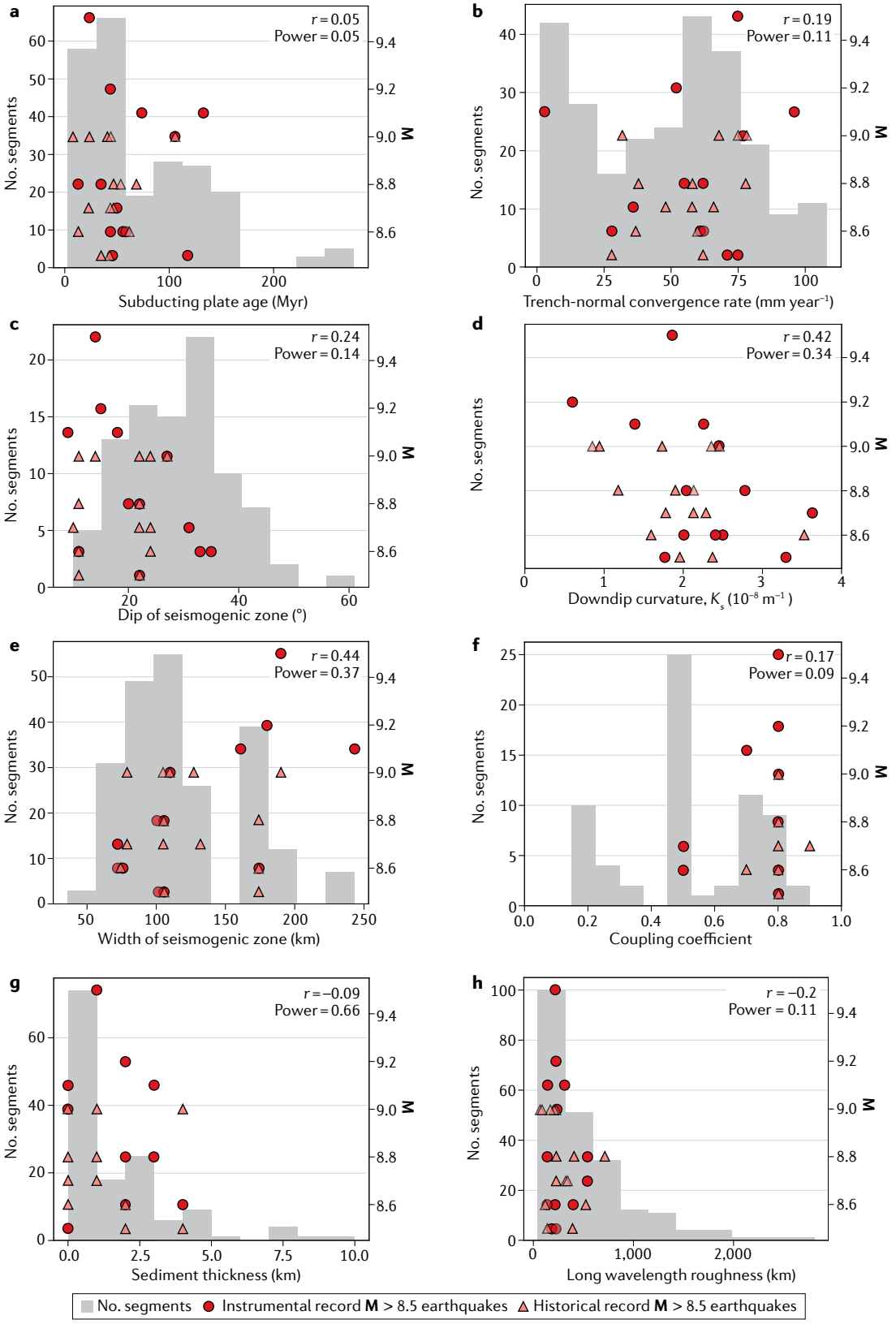

and properties of the overlying plate, which can vary widely between subduction systems (TABLE 1).

Caution must be taken in drawing sweeping conclusions regarding the control of specific parameters on subduction zone earthquake occurrence. The relatively short observational record (since the early twentieth century) is dwarfed by the length of the earthquake cycle (often hundreds to thousands of years between great events), and thus does not sample the full range of possible megathrust earthquake behaviour. Surprises such

◀ Fig. 3 | **Correlation between subduction zone parameters and the magnitude of great earthquakes.** Subduction zone parameters at individual segments identified as having hosted moment magnitude **M** ≥ 8.5 earthquakes in the instrumental (red circles) or historical (pink triangles) record, as well as the global distribution of those parameters (grey bars). Plots compare plate age (panel **a**), convergence rate (in the HS3-NUVEL1A absolute reference frame)[183] (panel **b**), dip of the seismogenic zone (panel **c**), downdip slab curvature (panel **d**), width of the seismogenic zone (panel **e**), coupling coefficients (panel **f**), sediment thickness (panel **g**) and long wavelength (80–100 km) roughness (panel **h**) with the historical and instrumental records of **M** ≥ 8.5 earthquakes. Data in panels **a**–**c**,**e**,**g** and **h** are from a continually updated subduction database[100] (http://submap.gm.univ-montp2.fr/). Parameters of global distributions are sampled at an interval of 2° along each subduction zone[100]. Downdip slab curvature values in panel **d** are from REF.[69], averaged over the rupture areas of events presented herein. Coupling coefficients in panel **f** are based on REF.[184] and averaged over subduction zone segments that share similar properties but are of differing megathrust lengths[184]. Correlation coefficient (*r*) and statistical power (the probability of a true positive result assuming a significance level of 0.05) between the individual parameter values and estimated earthquake magnitudes are given in the upper-right corner. In general, the statistical power values are low (well below the desired level of 0.8 or 80%), because of the weak correlation coefficients and/or small sample sizes. Data emphasize the need for continued study of earthquakes and their associated physical processes to draw any strong conclusions about links between earthquake occurrence and subduction zone structure.

as the 2004 **M**9.1 Sumatra–Andaman and 2011 **M**9.1 Tohoku earthquakes will continue to occur. Moreover, we have yet to fully understand the complex feedback between the many possible subduction parameters that contribute to the observed seismic behaviour.

Subduction zone geometry. Data compilations show that parameters related to subduction zone geometry — namely, the dip and curvature of the seismogenic zone — might influence rupture propagation and, therefore, the ability of a particular subduction zone to host large earthquakes (FIG. 3c,d). In general, a shallow slab dip angle tends to push the thermally controlled brittle-to-ductile transition to distances farther away from the trench, thus widening the seismogenic zone. Global correlations between subduction zone parameters and the size of megathrust earthquakes show that recorded earthquakes with **M** ≥ 8.5 have only occurred in subduction zones dipping <35° and with seismogenic zone widths >75 km. Similarly, recorded earthquakes with **M** ≥ 9.2 have only occurred in subduction zones dipping <20° and with seismogenic zone widths >150 km (REFS[66,67]). In aggregate, observational data suggest a relatively high correlation coefficient and statistical significance between seismogenic zone width and earthquake magnitude compared with other subduction zone parameters (FIG. 3e). Numerical models have also supported the observation that large earthquakes might be more likely to occur in the widest seismogenic zones[64,68].

The along-dip curvature of the subduction zone interface has also been noted as a possible control on the spatial extent of rupture, with the largest megathrust earthquakes associated with broadly planar fault interfaces[69,70] (FIG. 3d). Better correlations have been noted between maximum earthquake magnitude and downdip curvature than with slab dip angle[69]. Compared with other subduction zone parameters (FIG. 3), the average downdip curvature tends to show one of the highest correlation coefficients and statistical significance, with increased downdip curvature resulting in lower-event magnitudes. This correlation between average downdip curvature and maximum magnitude might be because small changes in the curvature of the slab produce only small gradients in shear strength, and that the critical shear stress is more likely to be exceeded over a broad area of the fault if the shear strength is relatively low and homogeneously distributed. However, it has also been noted that multiple subduction zones with a high degree of planarity are not known to have hosted a great earthquake, implying that the historical records in these regions are too short for such an event to have been observed, or that other subduction parameters might be exerting controls on megathrust rupture[70].

Similarly, the along-strike curvature of the subduction zone has also been suggested to influence the maximum magnitude of megathrust earthquakes. Large earthquakes have not been recorded in subduction zones with dramatic along-strike curvature (for example, Scotia, Marianas), which is thought to limit the rupture length[66,69]. Along the Chilean megathrust, the distribution of coseismic slip during both the 2010 **M**8.8 Maule and 2014 **M**8.2 Iquique earthquakes appears to be influenced by changes in curvature along the Andean subduction zone[26,71].

Sediments and plate roughness. The thickness of sediments entering the subduction zone on the incoming plate might also influence megathrust earthquake rupture[72,73] (FIGS 2,4). Thick sediments (>1 km) at the trench have been correlated with observations of large-magnitude earthquakes in subduction zones[72,73] (FIG. 3g). It is thought that the presence of subducted sediments, often inferred from the thickness of sediments at the trench, will smooth and lubricate the interface, promoting more homogeneous stress conditions and a low coefficient of friction on the fault, thus increasing the likelihood of rupturing a wide area of the megathrust[67,74,75]. However, it should be noted that trench-fill thickness does not necessarily represent sediment thickness along the plate boundary itself, as not all of this sediment is subducted[76].

In addition, it is expected that a relatively smooth, thickly sedimented subducting seafloor can result in a large zone of interseismic coupling, compared with a megathrust with a more heterogeneous coupling distribution owing to rough subducting topography[77,78] (FIG. 3f). A notable exception to the potential relationship between sediment thickness and great earthquakes is the **M**9.1 Tohoku earthquake at the northern Japan Trench, where the incoming plate is sediment-starved. However, the incoming seafloor in this region is suggested by some to be relatively smooth despite the lack of overlying sediment[72,76,79].

Somewhat related to the presence of subducting sediments, numerous studies have focused on the impact of incoming plate roughness on megathrust slip behaviour (FIGS 2,3h). Observations indicate a correlation between high interseismic coupling and low incoming plate roughness[76,77,80]. This correlation is in contrast to earlier studies assuming that geometric roughness provided an asperity for the generation of

Coupling
A quantitative value that can be determined geodetically, indicating the fraction of plate motion that is accommodated seismically.

Interseismic coupling
When a fault is locked or coupled due to friction along the plate boundary, leading to the accumulation of elastic strain that is ultimately released during an earthquake. Faults can be either fully locked or partially locked, or can creep aseismically with no interseismic coupling.

Table 1 | **Subduction zone parameters at selected margin segments**

Margin	Year	Magnitude	Event name	Curvature (downdip)[a]	Dip (°)	Seismogenic zone width (km)	Plate age (Myr)	Sediment thickness (km)	Long wavelength plate roughness (km)	Trench-perpendicular convergence rate (mm year^{-1})[b]	Coupling coefficient[c]
Japan (Honshu)	2011	9.1	Tohoku	1.39	18	161	132	<0.5	139 (smooth)	96	0.7
Cascadia	1700	9	Cascadia	0.94	11	127	7	4	76 (smooth)	32	0.8
Chile	2010	8.8	Maule	2.04	22	105	34	2	138 (smooth)	62	0.8
	1960	9.5	Valdivia	1.86	14	190	23	1	215 (smooth)	75	0.8
	1922	8.5	Atacama	1.77	22	105	45	<0.5	188 (smooth)	75	0.8
Alaska–Aleutians	1965	8.7	Rat Islands	3.63	31	72	49	–	536 (intermediate)	36	0.5
	1964	9.2	Alaska	0.6	15	180	43	2	223 (smooth)	52	0.8
	1957	8.6	Alaska	2.5	35	75	55	2	214 (smooth)	61	0.5
	1946	8.6	Unimak Island	2.41	33	72	57	–	145 (smooth)	62	0.5
Sumatra–Java	2005	8.6	Nias–Simeulue	2.01	11	174	43	4	391 (intermediate)	28	0.8
	2004	9.1	Sumatra–Andaman	2.26	9	243	73	3	307 (intermediate)	3	0.7
Kuril–Kamchatka	1963	8.5	Kuril Islands	3.31	22	102	117	<0.5	224 (smooth)	71	0.8
	1952	9	Kamchatka	2.45	27	110	105	<0.5	234 (smooth)	77	0.8
Ecuador–Colombia	1906	8.8	Ecuador–Colombia	2.78	20	101	12	3	538 (intermediate)	55	0.8

Subduction zone parameters for margin segments that have hosted observationally recorded megathrust earthquakes with moment magnitude **M** ≥ 8.5, as well as the Cascadia subduction zone which has robust historical records of tsunami inundation in Japan and palaeoseismic evidence for an **M**8.7–9.2 megathrust earthquake in 1700 AD[170,188,189]. An expanded version of this table that includes historical earthquakes and additional parameters is provided in Supplementary Data (additional information on the parameters and data sources is provided in Supplementary Note 1). Most of the parameters were obtained from the continually updated subduction database[100] (http://submap.gm.univ-montp2.fr/). [a]Downdip curvature values are from REF.[69]. [b]Trench-perpendicular convergence rate is in the HS3-NUVEL1A absolute reference frame[183]. [c]Average coupling coefficients are from REF.[184].

large earthquakes[81,82]. As a more localized form of plate roughness, subducting topographic relief (for example, subducting seamounts) (FIG. 2) are expected to result in complex forearc structure[83] and heterogeneous stresses that might be favourable to aseismic creep and small earthquakes, but unfavourable for the propagation of large earthquakes[77,84].

Seismic imaging and ocean drilling from the slow slip and creep-dominated northern Hikurangi subduction zone suggest that rough subducting crust can promote a lithologically and rheologically heterogeneous plate boundary fault[85]. Numerical modelling suggests that such heterogeneity will promote transient SSEs, rather than large, seismic slip[86–88]. However, a counterexample to the concept of geometric heterogeneities acting as a barrier to rupture is the 2007 **M**8.1 Solomon Islands earthquake that ruptured across a spreading centre with abundant adjacent seamounts, demonstrating that complex geometrical barriers can be bridged during a seismic event[89]. The 1730 ~**M**9 earthquake in Central Chile, which ruptured across a seamount ridge[90] and involved slip on both accretionary (>1 km of trench sediments) and erosive (<300 m of trench sediments) segments of the margin[91], is another example that emphasizes the secondary role of seamounts and other features as potential barriers to rupture.

Upper-plate characteristics. The upper plates of subduction zones are commonly associated with complex geological structures resulting from changes in boundary conditions over millions of years of plate convergence. By using gravity anomalies as a proxy for rock density, subduction zone forearc structure is suggested to exhibit a certain degree of correlation with areas of large coseismic slip during megathrust earthquakes[92–94]. Of the **M** ≥ 9 earthquakes (FIG. 5; TABLE 1) that occurred in the twenty-first century, the 2011 Tohoku event had the largest average slip and smallest rupture area. By correlating offshore gravity anomalies with onshore geology in this region of the Japan Trench, it has been proposed that a sharp along-strike gradient in the density of upper-plate rocks across a major continental fault zone resulted in the localization of interseismic plate locking, and thus coseismic slip, to a relatively small area[94]. Such a variability in forearc geology might have also controlled the slip distribution of other giant earthquakes, which are associated with distinct forearc terranes (for example, the 1700 Cascadia[95], 1960 Chile[96] and 2004 Sumatra–Andaman[97] earthquakes).

The strain regime across upper plates of subduction zones has long been suggested to correlate with the seismic behaviour on the megathrust[98–100] and the distribution of interseismic locking[101]. Margins with extensional

upper plates appear to have fewer great earthquakes, and in some cases host aseismic creep[102]. Various mechanisms have been suggested to explain this apparent correlation, including the possible influence of slab rollback on the interface stress state[99], and possible upper-plate tectonic stress state controls on permeability, fluid pressure and depth to the brittle-to-ductile transition[103]. However, the **M**9.1 Sumatra–Andaman earthquake was a notable counterexample to these correlations, as a substantial portion of its rupture area was adjacent to the Andaman back-arc rift[104].

In general, forearc strain has been correlated with subduction mode (that is, erosive or accretionary), as erosive margins are mostly associated with extension across the marine forearc (or portions of the forearc that overlie the megathrust seismogenic zone)[105]. Whereas contraction and development of fold-and-thrust belts are common across accretionary margins[105].

The strain regime across marine forearcs has been correlated with spatial patterns of slip during great earthquakes and is therefore relevant to seismic hazard[106]. Upper-plate strain is mostly accounted for by faults and folds, which are ubiquitous across subduction zone forearcs, and whose kinematics might reflect spatial variations in the frictional structure and seismogenic behaviour of the underlying megathrust[107]. For example, the large slip gradients during the 2011 **M**9.1 Tohoku earthquake were accommodated by anelastic extension across a mid-slope terrace evidenced by normal faults rupturing to the seafloor, and by anelastic contraction across thrusts rupturing the trench floor[10,108]. Therefore, mapping the distribution and characteristics of upper-plate faults is important, as they might reveal changes in the frictional structure of the underlying megathrust. In addition, several upper-plate faults have slipped during or shortly after great earthquakes[109,110], and therefore can pose a secondary shaking and tsunami hazard at the local to regional scale.

Taken together, it appears that the stronger controls on great megathrust earthquake occurrence are linked to the potential for rupture continuation: greater seismogenic zone width, less downdip curvature and, to some degree, smaller along-strike curvature. A wider, more uniform along-strike and downdip geometry seems to create more preferable conditions to achieve large spatial extents of high slip, increasing the chances of producing a great event. Numerous other characteristics such as the plate convergence rate, incoming sediment thickness, plate roughness and upper-plate structure likely exert secondary (but still significant) controls on large earthquake occurrence. Nonetheless, all of the above should still be considered with caution, given the lack of a statistically significant data set capturing the possible range of great earthquake occurrence during instrumental times.

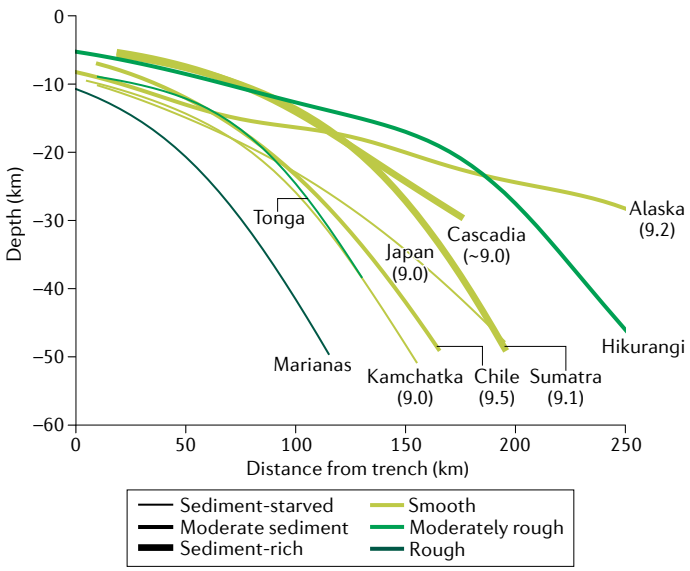

Fig. 4 | **Representative cross sections of global seismogenic zone geometries.** Transects[185] coloured according to a segment's average long wavelength (80–100 km) roughness on the incoming plate[76] and line width corresponding to estimates of sediment thickness at the trench (where thicker lines indicate sediment-rich systems and thin lines represent sediment-poor margins). The Japan, Kamchatka, Tonga and Marianas subduction systems are sediment-starved[102]. For subduction zones with a robustly constrained moment magnitude ~**M** ≥ 9.0 earthquake in the instrumental or historical record, the estimated magnitude of the largest event is given in parentheses. This figure demonstrates that there are various subduction zone geometries and characteristics capable of hosting great megathrust earthquakes.

Great earthquake hazards

In this section, the factors that influence seismic hazard (rupture characteristics and earthquake recurrence) and the earthquake source parameters that impact tsunami hazard are discussed. The earthquake rupture characteristics that control ground shaking and tsunamigenesis are distinct. In general, the shaking that impacts the built environment stems from higher-frequency ground motions (>0.1 Hz), and often originates in the downdip portions of the rupture zone. By contrast, tsunamigenesis is largely controlled by coseismic displacements of the seafloor above the shallow, offshore portion of the megathrust, as well as by the shape of local near-shore bathymetry and coastal morphology. Although cascading hazards such as landslides and liquefaction will also be impacted by the severity and duration of ground shaking, they also heavily depend on local site conditions (topography, lithology and shallow soil properties), which will vary locally and regionally[6,111,112].

Seismic hazard

Seismic hazard estimates require knowledge of how frequently earthquakes are expected to occur (recurrence intervals) and the anticipated ground shaking associated with those earthquakes. In addition to earthquake magnitude, numerous other rupture characteristics are known to influence the intensity of ground shaking and resulting seismic hazard[113]. These include the direction of rupture (because of rupture directivity effects), the downdip limit of rupture (which often controls the proximity of the rupture to inland cities and the polarity of coastal land-level changes), the earthquake rupture velocity, the location of strong motion-generating areas on the fault and, to some degree, earthquake stress drop[114,115].

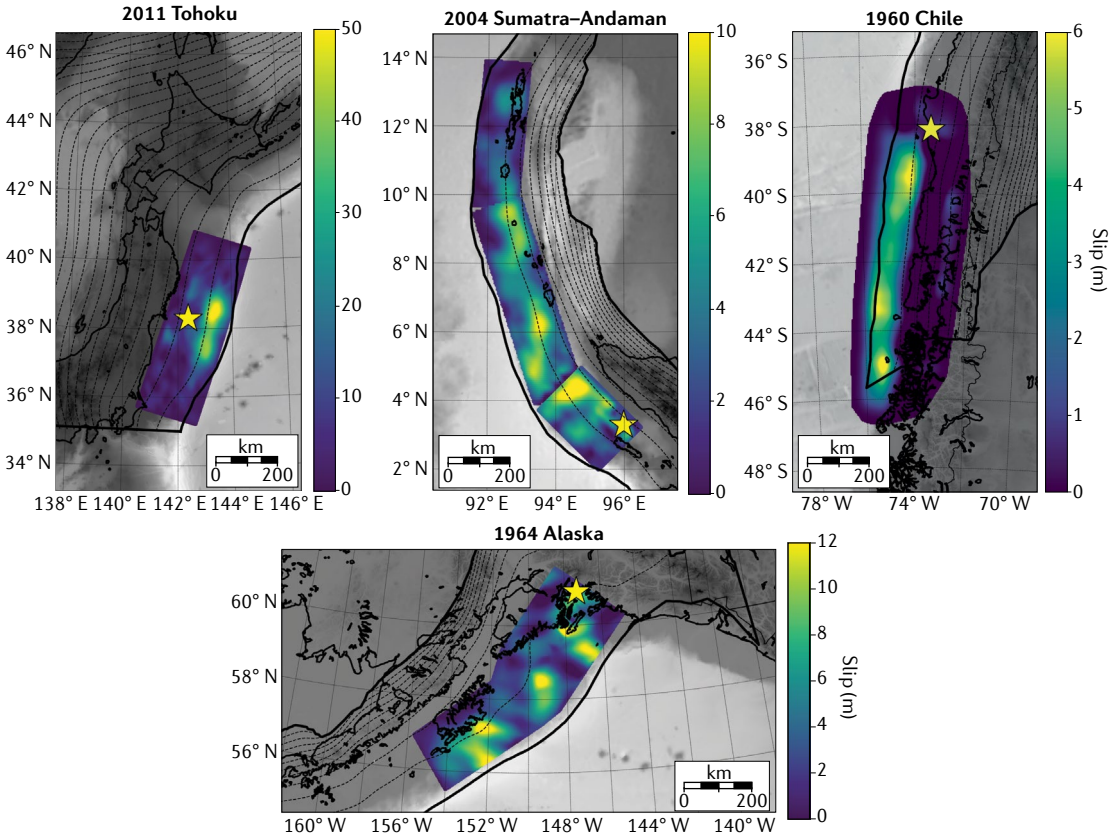

Fig. 5 | **Slip distributions from observations of giant megathrust earthquakes.** Slip estimates from the 1960 Chile[186], 1964 Alaska[187], 2004 Sumatra–Andaman[132] and 2011 Tohoku[177] earthquakes. Epicentres denoted by yellow stars. Slab contours from REF.[185] are plotted every 20 km. All dimensions in kilometres, to facilitate direct comparison. Slip patterns of instrumentally recorded great earthquakes are highly heterogeneous, both in the spatial distribution of slip as well as the width and length dimensions of the rupture. More compact ruptures tend to produce higher slip, to achieve the same magnitude.

Rupture directivity. The rupture extent and location of the hypocentre will control rupture directivity effects, which result in stronger-intensity ground shaking in the direction of fault rupture[116]. Earthquakes that rupture unilaterally and/or over a long along-strike rupture extent will likely induce stronger rupture directivity effects. Unilateral, along-strike rupture can also increase the duration of shaking compared with bilateral rupture (assuming roughly similar fault lengths). Longer-duration shaking is known to increase hazard and risk via building performance and, in some cases, increases structure collapse probabilities by nearly 30%[117]. Given that the majority of the seismogenic portion of the megathrust is typically located offshore, most populated regions tend to be located downdip of the megathrust (with some exceptions). Hypocentres that originate in the updip portion of the fault can therefore produce a substantial portion of rupture directed downdip towards sites on land.

Understanding patterns in hypocentre location for subduction zone earthquakes is thus important for constraining hazard estimates. Analyses of hypocentre location produce various hypotheses, including possible preferences for the along-strike and along-dip location of hypocentres[118–120]. Finite fault models for $\mathbf{M} \geq 7$ earthquakes in varying tectonic regimes revealed a slight preference for hypocentres to originate in the bottom half of the seismogenic zone, and a tendency for along-strike bilateral ruptures[120]. However, when examining only the largest ($\mathbf{M} \gtrsim 9$) subduction zone megathrust earthquakes, there appears to be some tendency towards unilateral ruptures[121], which may increase rupture directivity effects and shaking duration (FIG. 5).

Stress drop and short-period radiation. The spatial distribution of high-frequency radiation is critical to hazard analyses, as the fundamental periods of many structures in the built environment are fairly short. Single-storey to 20-storey structures are expected to have fundamental periods of ~0.05–2.0 s, and therefore ground shaking at these short periods can result in increased structural damage. Earthquake stress drop controls the amount of radiated seismic energy, and thus the amplitude and frequency content of ground shaking[114,122,123]. Stress drop is considered to be independent of earthquake magnitude, but can vary regionally[124,125] and with depth[12,126]. Great earthquakes in the twenty-first century (for example, the 2010 Maule and 2011 Tohoku events) have also been characterized by higher than average stress drops, possibly suggesting higher friction coefficients and/or higher effective normal stresses compared with smaller events[66]. In well-imaged large megathrust earthquakes, it appears

Rupture directivity
The focusing of seismic energy in the direction of fault rupture, leading to stronger ground shaking in the direction of rupture propagation.

that the most substantial short-period radiation originates from distinct patches in the downdip region of the fault, potentially because of the higher stresses at depth[32].

During the 2011 **M**9.1 Tohoku earthquake, the strongest ground motions appeared to originate from individual patches on the deeper portion of the megathrust, resulting in distinct wave packets or pulses in the recorded waveforms. These were termed 'strong motion generating areas'[44,45] and 'high stress drop subevents'[46]. These strong motion-generating areas were located separate from and downdip of the largest slip asperity, and were roughly equivalent to ~**M**8–8.5 earthquakes[46]. Their location on the megathrust is similar to that of smaller magnitude (~**M**3–5) repeating earthquakes (that is, events that repeatedly rupture the same fault patch), which have been well documented in northeast Japan[126,127]. Additionally, the portions of the 2011 Tohoku rupture that radiated more high-frequency energy tended to correspond to areas of higher stress drop in small seismicity, with an overall increase in stress drop with depth between 30 and 60 km depth in the Japan Trench[126].

Rupture velocity. Rupture speed describes how fast the rupture expands, but it can be difficult to determine. Numerical modelling suggests that higher rupture velocities result in stronger ground shaking, and thus increased seismic hazard, by concentrating energy towards the rupture front[128]. In addition, some works have shown that supershear ruptures produced higher-observed ground motions[129]. Observations suggest that large dip-slip earthquakes appear to rupture more slowly (~1–3 km s^{-1}) than large strike-slip events, staying well below the shear wave speed[130]. Tsunami earthquakes tend to have the lowest rupture velocities, typically <1 km s^{-1} (REF.[131]).

Of the twenty-first-century large megathrust earthquakes, the 2004 Sumatra–Andaman earthquake had an estimated rupture velocity of 2–3 km s^{-1} (REF.[132]), the 2010 Maule earthquake ruptured at speeds around 2.0–2.6 km s^{-1} (REFS[133,134]) and the 2011 Tohoku earthquake initially ruptured slowly (~1 km s^{-1}), accelerating to 2–3 km s^{-1} as the rupture progressed[135,136]. In general, faster ruptures tend to occur on long, straight segments of the fault, with low friction and no barriers to rupture[129,137]. Two-dimensional dynamic simulations suggest that whereas supershear ruptures are more likely to occur on rough faults (because of the variety of rupture styles they can induce), sustained fast rupture tends to favour smoother fault segments[138].

Downdip rupture limit. The location of the downdip extent of the seismogenic zone (approximately shallower than the location of the SSE in FIG. 2) often dictates the proximity of a megathrust earthquake rupture to populated inland regions. Ground motions are heavily dependent on the distance between the earthquake and site of interest, with shaking decreasing as a function of distance. Therefore, the downdip extent of rupture exerts a first-order control on shaking intensity, because a rupture extent that is further inland will be closer to onshore population centres. In many subduction zones, the downdip extent of rupture also controls the polarity of coastal land-level change (the regions that experience coseismic uplift versus subsidence)[139]. The downdip extent of rupture, in turn, has important implications for coastal morphology and tsunami inundation, by either decreasing or increasing the potential tsunami run-up, respectively.

Global compilations have found a potential correlation between the downdip width of the seismogenic zone and the occurrence of **M** ≥ 8.5 earthquakes[140]. Many recorded great earthquakes have occurred on the flattest and widest subduction zones[140], with the narrow and fairly steep (dip angle ~30–35°) Aleutian arc as an important exception (Supplementary Data). However, because seismic moment is directly related to the rupture area, subduction zones with a shallow slab dip (and thus a possibly wider seismogenic zone) might have greater potential for large earthquake moment release, which in general will increase ground motions.

Earthquake recurrence. In addition to the earthquake source characteristics that influence the strength of ground shaking, a critical component impacting seismic hazard is where and how often great subduction zone earthquakes occur. Megathrust earthquake palaeoseismology is inherently different from crustal earthquake palaeoseismology, because it relies on off-fault proxies for regional deformation and shaking, as opposed to directly sampling the fault zone. These proxies include estimates of coastal land-level change, tsunami inundation and/or ground shaking (such as turbidites and lacustrine deposits), and their spatial and temporal information is used to define past rupture limits and recurrence intervals[141–144].

Advances in subduction zone palaeoseismology have led to long and detailed records of past seismic cycles at some subduction zones, with the longest archives extending back several millennia[20]. These records have associated uncertainties spanning several decades to a century, which propagate into hazard estimates. Higher temporal resolution has been provided by the analysis of growth patterns in coral microatolls along the Sumatran subduction zone, providing detailed histories of land-level changes between and during earthquakes spanning multiple seismic cycles[22]. This work revealed clustered earthquakes of different magnitudes separated by long periods of strain accumulation, termed supercycles. Subsequent studies integrating both palaeoseismic archives and historical records suggest that supercycle behaviour or superimposed cycles might be a hallmark of many subduction zones[20,145]. Long palaeoseismic archives spanning several thousand years, but that record only the largest events at a single segment of a subduction zone, show more periodic behaviour[143].

Numerical models have related supercycle behaviour to changes in the width of the seismogenic zone[68] or to spatial changes in frictional properties of the megathrust[146]. The latter has also been proposed by analogue modelling experiments[147]. For hazard estimates, supercycle behaviour is more important than the choice of probability density function used to characterize

Supershear ruptures
Earthquakes in which the rupture velocity is faster than the shear wave (S wave) speeds of the host rock.

Supercycles
Broad periods of strain accumulation followed by a temporal cluster of differently sized megathrust earthquakes, ultimately leading to the complete failure of a subduction zone segment.

Superimposed cycles
Long-term cycles of strain accumulation and release, overlapping in both space and time with a short-term cycle of strain accumulation and release on the same fault.

recurrence times[148], because the knowledge of whether a region is in or outside a long-term cluster can change probabilistic hazard estimates in comparison with assuming simply periodic behaviour. However, modelling supercycle behaviour requires the use of hazard models that consider time-dependent hazard in terms of strain accumulation over longer periods of time, rather than simply considering the time elapsed since the last earthquake.

Despite the wealth of information provided by palaeoseismic studies, the record remains less complete than the modern instrumental record. Some regions are not conducive to recording or preserving all geologic proxies of earthquakes[149,150], whereas in other regions palaeoseismic archives have provided evidence for larger earthquakes than historical catalogues[151]. This disparity in geologic proxy formation or preservation presents a challenge in capturing the full range of where great earthquakes have occurred, as well as their size and timing.

Tsunami hazard

Great subduction zone earthquakes also represent a substantial tsunami hazard. Several main characteristics control the occurrence and amplitude of tsunamis: the magnitude of seafloor deformation, the heterogeneity of slip and resulting seafloor deformation, the velocity with which the seafloor moves during the event and, to some degree, the mechanical properties of the seafloor sediments.

Shallow (less than ~15 km) coseismic slip is arguably the greatest factor impacting tsunamigenesis; greater amounts of shallow slip produce larger seafloor displacements and larger tsunami amplitudes[152,153]. In addition to vertical seafloor deformation, some modelling and observational work has demonstrated that horizontal displacement of steep bathymetry can enhance tsunamigenesis[154,155] and, thus, oblique and/or strike-slip dominated ruptures can also produce tsunamis. Finally, strong ground motions produced in large earthquakes can trigger submarine landslides on continental slopes, resulting in greater tsunami amplitudes. This mechanism has been proposed for the large tsunami amplitudes observed during the 2011 Tohoku event[156], but is not strictly required[11].

Although larger amounts of shallow slip tend to create higher tsunami amplitudes, it has also been shown that heterogeneous rupture with large amounts of peak slip over a smaller area can have a substantial impact on increasing local tsunami amplitudes and run-up[157]. In addition to the amount of slip, the rupture and geometry of shallow splay faults in the outer forearc (FIG. 2) could also play an important role in generating larger tsunami amplitudes than the megathrust alone. Splay faults that branch off from the megathrust typically have steep dip angles that result in increased vertical deformation and larger tsunamis[158,159]. Although splay faults are proposed as a mechanism for numerous tsunamigenic events[160–162], models of slip on the megathrust alone can often explain the observed tsunami amplitudes. The significance of splay faulting in increasing tsunami amplitudes remains unresolved and should be improved with future observations.

Slow earthquake rupture velocities, which are of the order of hundreds of metres per second and similar to the tsunami wave propagation velocity, have been postulated to enhance tsunami generation[163,164]. Such slow rupture velocities are highly uncommon for most megathrust ruptures, but are characteristic of some tsunami earthquakes[163]. Average rupture velocities appear to have little to no impact on tsunami amplitudes and run-up in the near field, but unilateral rupture and variability in earthquake rupture velocity can rotate tsunami energy and the direction of propagation across ocean basins, thus influencing far-field tsunami impacts[165].

Lastly, although most models suggest that elastic deformation of the seafloor during the earthquake rupture exerts the primary control on tsunami generation, dynamic analyses have shown that efficient tsunami generation can be enhanced by inelastic deformation of the accretionary wedge[166]. In this scenario, shallow slip couples with inelastic wedge failure to produce large seafloor deformation, indicating that shallow sedimentary wedge properties can influence tsunamigenesis.

The earthquake source properties that impact seismic hazard do not necessarily impact tsunamigenesis, and thus tsunami hazard, in the same way. Tsunamigenesis is typically unaffected by the characteristics of the downdip portion of the rupture, and instead is controlled by the updip portion of the rupture, which creates greater seafloor deformation[167]. Therefore, shallow subduction zone characteristics such as the presence of splay faults, and shallow rupture characteristics such as large amounts of near-trench slip, are typically the more important parameters for tsunami hazard.

Summary and future perspectives

Given the sparse (and inherently short) instrumental earthquake records available to underpin probabilistic seismic and tsunami hazard analyses in subduction zones, establishing the primary physical characteristics that control the occurrence of great earthquakes is clearly desirable.

Numerous parameters have been suggested to influence the ability of a subduction zone to host great megathrust earthquakes, including the convergence rate; plate age and thermal state; large-scale geometry (along-strike and downdip); geometric and/or lithological heterogeneity on the megathrust; sediment thickness; and upper-plate characteristics. Yet major twenty-first-century subduction zone earthquakes have called into question long-standing assumptions about whether some of these parameters dictate the likelihood of subduction zones to host such devastating events. Given the complexity and diversity of subduction systems, it seems unlikely that a single physical parameter can satisfactorily explain global subduction zone earthquake occurrence and variability, and that multiple factors and the feedback between them must be considered. Developing a framework to evaluate the interplay between these factors, and harnessing this framework to inform knowledge of seismic and tsunami hazard, represents a major outstanding challenge.

Although determining the ability of a particular subduction zone segment to host great earthquakes is critically important, there are numerous other factors that contribute to the resulting seismic and tsunami hazard estimates. For example, knowing the extent (updip and downdip limits) and spatial distribution of slip is critical to estimating the intensity and frequency content of strong ground motions, as well as the tsunamigenic potential of an event. Yet predicting potential future spatial distributions of slip is fraught with uncertainties. Estimates of earthquake slip distributions can be based on the interseismic coupling determined from geodetic methods. However, such coupling will not account for the possibility that some of the interseismic strain accumulation can be released heterogeneously and/or aseismically. It also cannot account for the possibility that 'stress shadows', or areas adjacent to a locked region where the degree of stress accumulation is low (or uncertain), might still be capable of being pushed to failure during adjacent seismic rupture[168]. Similarly, the distribution of interseismic locking might change over time, and not be adequately represented in coupling models[169]. In addition, locking on the shallow (<20 km depth) megathrust is typically poorly constrained due to the absence of offshore geodetic data at most subduction zones, which exacerbates the uncertainties in estimating future coseismic slip. Improved knowledge of offshore megathrust slip behaviour, and the seaward extent and shallow geometry of possible rupture, is critically needed to reduce uncertainties in tsunami hazard models.

Addressing the earthquake potential of the shallow, tsunamigenic portions of megathrusts is one of the most challenging frontiers and requires widespread application of multi-proxy techniques to undertake permanent offshore monitoring. This infrastructure could include seafloor geodetic measurements, and cabled networks of offshore geophysical sensors to resolve crustal deformation and seismicity at many of the world's subduction zones. For probabilistic hazard estimates, another outstanding issue is the definition of appropriate magnitude-frequency distributions (Gutenberg–Richter versus characteristic models), which appear to vary greatly among subduction zones[70]. Parameters such as the maximum magnitude and *b*-value (which determines the relative proportion of small versus large earthquakes) are also necessary to define, but difficult to establish given the deficiencies in global earthquake catalogues.

Overall, the most robust way of improving incomplete understanding of the earthquake and tsunami potential of global subduction zones is through refined palaeoseismic studies in tandem with modern technologies. These approaches include sustained seismological and geodetic monitoring across the entirety of the seismogenic zone — both onshore and offshore — over multiple earthquake cycles. Although comprehensive palaeoseismic archives have extended the subduction earthquake record in some locations[142,143,170], there are still large uncertainties in the interpretation of these data sets with regards to earthquake magnitude, timing and rupture characteristics. Modern high-resolution geochronological techniques will allow further exploitation of the palaeoseismic record, and the linking of observations at multiple sites to a single earthquake event[171]. Additionally, where available, spatially linking geologic proxies for shaking with geotechnical studies can be used to constrain both the palaeoseismic record as well as shaking estimates[149]. Although high in uncertainty, estimating shaking from proxies might help to tease apart megathrust sources from intra-slab and crustal sources in subduction zones[172], which is critical for seismic hazard modelling.

Shoreline-crossing continuous geophysical monitoring will provide much-needed constraints on basic earthquake processes that will improve the understanding of subduction zone hazards. Offshore instrumentation will lower the magnitude of completeness in earthquake catalogues and resolve additional small earthquakes, enabling analogue studies for large earthquake source processes using smaller seismicity. Simultaneously, this instrumentation can improve the imaging resolution of large earthquake sources when they occur. Improved resolution of earthquake sources will allow further constraints on the characteristics of spatially variable rupture parameters, such as strong motion-generating areas and shallow tsunamigenic slip during future large earthquakes. In addition, sustained geophysical monitoring will improve the understanding of magnitude-frequency distributions, potentially provide observations of precursory signals and migrating foreshock sequences, and identify interactions between seismic and aseismic slip.

Geophysical and palaeoseismic observations of earthquake sources will be most powerful when integrated with data elucidating the physical properties, structure and hydrogeology of the plate boundary. For example, seismic, electromagnetic and magnetotelluric imaging, scientific ocean drilling and rock deformation experiments help reveal the physical processes underlying subduction zone earthquake occurrence. Furthermore, these observations should be used to both underpin and validate numerical models. Numerical models spanning multiple seismic cycles — from interseismic deformation through to dynamic rupture — can fill in data gaps to investigate how the variety of subduction slip behaviours interact in space in time, and the impact of spatio-temporal slip behaviour on seismic hazard. Large, concerted community exercises to validate modelling codes and methods are important to vet and port model findings to hazard applications[173]. Ultimately, the large uncertainties surrounding megathrust earthquakes and tsunami hazard are likely to be addressed many centuries into the future with sustained seismological and geodetic monitoring at subduction zones, coupled with multidisciplinary investigations of the physical properties controlling earthquake occurrence on these major fault systems.

Data availability

Raw data behind all data synthesis can be found within Supplementary Data.

Published online: 18 January 2022

1. Telford, J. & Cosgrave, J. Joint evaluation of the international response to the Indian Ocean tsunami: synthesis report (Tsunami Evaluation Coalition, 2006).
2. *The 137th report* (FDMA, 2011); http://www.fdma.go.jp/bn/2011/detail/691.html
3. Kajitani, Y., Chang, S. E. & Tatano, H. Economic impacts of the 2011 Tohoku-Oki earthquake and tsunami. *Earthq. Spectra* **29**, 457–478 (2013).
4. Reid, H. F. in *The California Earthquake of April 18, 1906: Report of the State Investigation Commission* Vol. **2** (Carnegie Institution of Washington, 1910).
5. Briggs, R. W. et al. Deformation and slip along the Sunda megathrust in the great 2005 Nias-Simeulue earthquake. *Science* **311**, 1897–1901 (2006).
6. Wartman, J., Dunham, L., Tiwari, B. & Pradel, D. Landslides in eastern Honshu Induced by the 2011 Tohoku earthquake landslides in eastern Honshu induced by the 2011 Tohoku earthquake. *Bull. Seismol. Soc. Am.* **103**, 1503–1521 (2013).
7. Verdugo, R. & González, J. Liquefaction-induced ground damages during the 2010 Chile earthquake. *Soil. Dyn. Earthq. Eng.* **79**, 280–295 (2015).
8. Fraser, S. et al. Tsunami damage to coastal defences and buildings in the March 11th 2011 M w 9.0 Great East Japan earthquake and tsunami. *Bull. Earthq. Eng.* **11**, 205–239 (2013).
9. *The Human Cost of Natural Disasters 2015: A Global Perspective* (CRED, 2015).
10. Kodaira, S. et al. Coseismic fault rupture at the trench axis during the 2011 Tohoku-Oki earthquake. *Nat. Geosci.* **5**, 646–650 (2012).
11. Lay, T. A review of the rupture characteristics of the 2011 Tohoku-Oki Mw 9.1 earthquake. *Tectonophysics.* **733**, 4–36 (2018).
12. Bilek, S. L. & Lay, T. Subduction zone megathrust earthquakes. *Geosphere* **14**, 1468–1500 (2018).
13. *Global Historical Tsunami Database* (NOAA, 2021); https://doi.org/10.7289/V5PN93H7.
14. Bock, Y. & Melgar, D. Physical applications of GPS geodesy: a review. *Rep. Prog. Phys.* **79**, 106801 (2016).
15. Moreno, M., Rosenau, M. & Oncken, O. 2010 Maule earthquake slip correlates with pre-seismic locking of Andean subduction zone. *Nature* **467**, 198–202 (2010).
16. Loveless, J. P. & Meade, B. J. Spatial correlation of interseismic coupling and coseismic rupture extent of the 2011 MW=9.0 Tohoku-Oki earthquake. *Geophys. Res. Lett.* **38**, L17306 (2011).
17. Protti, M. et al. Nicoya earthquake rupture anticipated by geodetic measurement of the locked plate interface. *Nat. Geosci.* **7**, 117–121 (2014).
18. Métois, M., Vigny, C. & Socquet, A. Interseismic coupling, megathrust earthquakes and seismic swarms along the Chilean subduction zone (38–18 S). *Pure Appl. Geophys.* **173**, 1431–1449 (2016).
19. Wesson, R. L., Melnick, D., Cisternas, M., Moreno, M. & Ely, L. L. Vertical deformation through a complete seismic cycle at Isla Santa Maria, Chile. *Nat. Geosci.* **8**, 547–551 (2015).
20. Philibosian, B. & Meltzner, A. J. Segmentation and supercycles: a catalog of earthquake rupture patterns from the Sumatran Sunda megathrust and other well-studied faults worldwide. *Quaternary Sci. Rev.* **241**, 106390 (2020).
21. Kelsey, H. M., Nelson, A. R., Hemphill-Haley, E. & Witter, R. C. Tsunami history of an Oregon coastal lake reveals a 4600 yr record of great earthquakes on the Cascadia subduction zone. *Geol. Soc. Am. Bull.* **117**, 1009–1032 (2005).
22. Sieh, K. et al. Earthquake supercycles inferred from sea-level changes recorded in the corals of west Sumatra. *Science* **322**, 1674–1678 (2008).
23. McCann, W. R., Nishenko, S. P., Sykes, L. R. & Krause, J. in *Earthquake Prediction and Seismicity Patterns* 1082–1147 (Birkhäuser, 1979).
24. Campos, J. et al. A seismological study of the 1835 seismic gap in south-central Chile. *Phys. Earth Planet. Inter.* **132**, 177–195 (2002).
25. Madariaga, R., Métois, M., Vigny, C. & Campos, J. Central Chile finally breaks. *Science* **328**, 181–182 (2010).
26. Moreno, M. et al. Toward understanding tectonic control on the Mw 8.8 2010 Maule Chile earthquake. *Earth Planet. Sci. Lett.* **321**, 52–165 (2012).
27. Kagan, Y. Y. & Jackson, D. Seismic gap hypothesis: ten years after. *J. Geophys. Res. Solid Earth* **96**, 21419–21431 (1991).
28. Jackson, D., Kagan, Y. Y. & Gupta, H. K. Characteristic earthquakes and seismic gaps. *Encycl. Solid Earth Geophys.* **5**, 1539 (2011).
29. Wyss, M. & Wiemer, S. in *Seismicity Patterns, Their Statistical Significance and Physical Meaning* (eds Wyss, M., Shimazaki, K. & Ito, A.) 259–278 (Birkhäuser, 1999).
30. Scholz, C. Earthquakes and friction laws. *Nature* **391**, 37–42 (1998).
31. Kato, A. & Ben-Zion, Y. The generation of large earthquakes. *Nat. Rev. Earth Environ.* **2**, 26–39 (2021).
32. Lay, T. et al. Depth-varying rupture properties of subduction zone megathrust faults. *J. Geophys. Res. Solid Earth* **117**, B04311 (2012).
33. Noda, H. & Lapusta, N. Stable creeping fault segments can become destructive as a result of dynamic weakening. *Nature* **493**, 518–521 (2013).
34. Ye, L., Lay, T. & Rivera, L. Rupture characteristics of major and great (Mw ≥ 7.0) megathrust earthquakes from 1990 to 2015: 2. Depth dependence. *J. Geophys. Res. Solid Earth* **121**, 845–863 (2016).
35. Morgan, P., Feng, L., Meltzner, A., Mallick, R. & Hill, E. Diverse slip behavior of the banyak islands subsegment of the sunda megathrust in Sumatra, Indonesia. *J. Geophys. Res. Solid Earth* **125**, e2020JB020011 (2020).
36. Bilek, S. & Lay, T. Rigidity variations with depth along interplate megathrust faults in subduction zones. *Nature* **400**, 443–446 (1999).
37. Sallarès, V. & Ranero, C. Upper-plate rigidity determines depth-varying rupture behaviour of megathrust earthquakes. *Nature* **576**, 96–101 (2019).
38. Boatwright, J. & Choy, G. Teleseismic estimates of the energy radiated by shallow earthquakes. *J. Geophys. Res. Solid Earth* **91**, 2095–2112 (1986).
39. Sahakian, V., Melgar, D. & Muzli, M. Weak near-field behavior of a tsunami earthquake: toward real-time identification for local warning. *Geophys. Res. Lett.* **46**, 9519–9528 (2019).
40. Kanamori, H. Mechanism of tsunami earthquakes. *Phys. Earth Planet. Inter.* **6**, 346–359 (1972).
41. Hill, E. et al. The 2010 Mw 7.8 Mentawai earthquake: very shallow source of a rare tsunami earthquake determined from tsunami field survey and near-field GPS data. *J. Geophys. Res. Solid Earth* **117**, B06402 (2012).
42. Kanamori, H. The diversity of large earthquakes and its implications for hazard mitigation. *Annu. Rev. Earth Planet. Sci.* **42**, 7–26 (2014).
43. Mai, P. & Beroza, G. A spatial random field model to characterize complexity in earthquake slip. *J. Geophys. Res. Solid. Earth* **107**, ESE–10 (2002).
44. Kurahashi, S. & Irikura, K. Short-period source model of the 2011 M w 9.0 off the Pacific coast of Tohoku earthquake. *Bull. Seismol. Soc. Am.* **103**, 1373–1393 (2013).
45. Kurahashi, S. & Irikura, K. Source model for generating strong ground motions during the 2011 off the Pacific coast of Tohoku earthquake. *Earth Planets Space* **63**, 11 (2011).
46. Frankel, A. Rupture history of the 2011 M 9 Tohoku Japan earthquake determined from strong-motion and high-rate GPS recordings: subevents radiating energy in different frequency bands. *Bull. Seismol. Soc. Am.* **103**, 1290–1306 (2013).
47. Dragert, H., Wang, K. & James, T. A silent slip event on the deeper Cascadia subduction interface. *Science* **292**, 1525–1528 (2001).
48. Schwartz, S. & Rokosky, J. Slow slip events and seismic tremor at circum-Pacific subduction zones. *Rev. Geophys.* **45**, RG3004 (2007).
49. Obara, K., Hirose, H., Yamamizu, F. & Kasahara, K. Episodic slow slip events accompanied by non-volcanic tremors in southwest Japan subduction zone. *Geophys. Res. Lett.* **31**, L23602 (2004).
50. Shelly, D., Beroza, G., Ide, S. & Nakamula, S. Low-frequency earthquakes in Shikoku, Japan, and their relationship to episodic tremor and slip. *Nature* **442**, 188–191 (2006).
51. Bartlow, N. M., Miyazaki, S. I., Bradley, A. M. & Segall, P. Space–time correlation of slip and tremor during the 2009 Cascadia slow slip event. *Geophys. Res. Lett.* **38**, L18309 (2011).
52. Wallace, L. & Beavan, J. Diverse slow slip behavior at the Hikurangi subduction margin, New Zealand. *J. Geophys. Res. Solid Earth* **115**, B12402 (2010).
53. Radiguet, M. et al. Slow slip events and strain accumulation in the Guerrero gap, Mexico. *J. Geophys. Res. Solid Earth* **117**, B04305 (2012).
54. Davis, E., Villinger, H. & Sun, T. Slow and delayed deformation and uplift of the outermost subduction prism following ETS and seismogenic slip events beneath Nicoya Peninsula, Costa Rica. *Earth Planet. Sci. Lett.* **410**, 117–127 (2015).
55. Wallace, L. et al. Slow slip near the trench at the Hikurangi subduction zone, New Zealand. *Science* **352**, 701–704 (2016).
56. Araki, E. et al. Recurring and triggered slow-slip events near the trench at the Nankai Trough subduction megathrust. *Science* **356**, 115 (2017).
57. Ito, Y. et al. Episodic slow slip events in the Japan subduction zone before the 2011 Tohoku-Oki earthquake. *Tectonophysics* **600**, 14–26 (2013).
58. Ruiz, S. et al. Intense foreshocks and a slow slip event preceded the 2014 Iquique Mw 8.1 earthquake. *Science* **345**, 1165–1169 (2014).
59. Vigny, C. et al. The 2010 Mw 8.8 Maule megathrust earthquake of central Chile, monitored by GPS. *Science* **332**, 1417–1421 (2011).
60. Lapusta, N. & Rice, J. Nucleation and early seismic propagation of small and large events in a crustal earthquake model. *J. Geophys. Res. Solid Earth* **108**, 2205 (2003).
61. Bilek, S., Schwartz, S. & DeShon, H. Control of seafloor roughness on earthquake rupture behavior. *Geology* **31**, 455–458 (2003).
62. Duan, B. Dynamic rupture of the 2011 Mw 9.0 Tohoku-Oki earthquake: roles of a possible subducting seamount. *J. Geophys. Res. Solid Earth* **117**, B05311 (2012).
63. Ruff, L. & Kanamori, H. Seismicity and the subduction process. *Phys. Earth Planet. Inter.* **23**, 240–252 (1980).
64. Corbi, F., Herrendörfer, R., Funiciello, F. & van Dinther, Y. Controls of seismogenic zone width and subduction velocity on interplate seismicity: insights from analog and numerical models. *Geophys. Res. Lett.* **44**, 6082–6091 (2017).
65. Oleskevich, D., Hyndman, R. & Wang, K. The updip and downdip limits to great subduction earthquakes: thermal and structural models of Cascadia, south Alaska, SW Japan, and Chile. *J. Geophys. Res.* **104**, 14965–14991 (1999).
66. Schellart, W. & Rawlinson, N. Global correlations between maximum magnitudes of subduction zone interface thrust earthquakes and physical parameters of subduction zones. *Phys. Earth Planet. Inter.* **225**, 41–67 (2013).
67. Muldashev, I. & Sobolev, S. What controls maximum magnitudes of giant subduction earthquakes? *Geochem. Geophys. Geosystems* **21**, e2020GC009145 (2020).
68. Herrendörfer, R., van Dinther, Y., Gerya, T. & Dalguer, L. Earthquake supercycle in subduction zones controlled by the width of the seismogenic zone. *Nat. Geosci.* **8**, 471–474 (2015).
69. Bletery, Q. et al. Mega-earthquakes rupture flat megathrusts. *Science* **354**, 1027–1031 (2016).
70. Plescia, S. & Hayes, G. Geometric controls on megathrust earthquakes. *Geophys. J. Int.* **222**, 1270–1282 (2020).
71. Shrivastava, M. et al. Earthquake segmentation in northern Chile correlates with curved plate geometry. *Sci. Rep.* **9**, 1–10 (2019).
72. Scholl, D. et al. Great (≥Mw8. 0) megathrust earthquakes and the subduction of excess sediment and bathymetrically smooth seafloor. *Geosphere* **11**, 236–265 (2015).
73. Ruff, L. in *Subduction Zones Part II* (eds Ruff, L. J. & Kanamori, H.) 263–282 (Birkhäuser, 1989).
74. Sobolev, S., Babeyko, A., Koulakov, I. & Oncken, O. in *The Andes* (eds Oncken, O. et al.) 513–535 (Springer, 2006).
75. Brizzi, S., Van Zelst, I., Funiciello, F., Corbi, F. & van Dinther, Y. How sediment thickness influences subduction dynamics and seismicity. *J. Geophys. Res. Solid Earth* **125**, e2019JB018964 (2020).
76. Lallemand, S., Peyret, M., van Rijsingen, E., Arcay, D. & Heuret, A. Roughness characteristics of oceanic seafloor prior to subduction in relation to the seismogenic potential of subduction zones. *Geochem. Geophys. Geosystems* **19**, 2121–2146 (2018).
77. Wang, K. & Bilek, S. Invited review paper: Fault creep caused by subduction of rough seafloor relief. *Tectonophysics* **610**, 1–24 (2014).
78. Collot, J. et al. Subducted oceanic relief locks the shallow megathrust in central Ecuador. *J. Geophys. Res. Solid Earth* **122**, 3286–3305 (2017).
79. Gao, X. & Wang, K. Strength of stick-slip and creeping subduction megathrusts from heat flow observations. *Science* **345**, 1038–1041 (2014).
80. van Rijsingen, E. et al. How subduction interface roughness influences the occurrence of large interplate earthquakes. *Geochem. Geophys. Geosystems* **19**, 2342–2370 (2018).

81. Cloos, M. Thrust-type subduction-zone earthquakes and seamount asperities: a physical model for seismic rupture. *Geology* **20**, 601–604 (1992).
82. Scholz, C. & Small, C. The effect of seamount subduction on seismic coupling. *Geology* **25**, 487–490 (1997).
83. Kopp, H. Invited review paper: The control of subduction zone structural complexity and geometry on margin segmentation and seismicity. *Tectonophysics* **589**, 1–16 (2013).
84. Wang, K. & Bilek, S. Do subducting seamounts generate or stop large earthquakes? *Geology* **39**, 819–822 (2011).
85. Barnes, P. M. et al. Slow slip source characterized by lithological and geometric heterogeneity. *Sci. Adv.* **6**, eaay3314 (2020).
86. Ando, R., Takeda, N. & Yamashita, T. Propagation dynamics of seismic and aseismic slip governed by fault heterogeneity and Newtonian rheology. *J. Geophys. Res. Solid Earth* **117**, B11308 (2012).
87. Skarbek, R., Rempel, A. & Schmidt, D. Geologic heterogeneity can produce aseismic slip transients. *Geophys. Res. Lett.* **39**, 21306 (2012).
88. Webber, S., Ellis, S. & Fagereng, Å. "Virtual shear box" experiments of stress and slip cycling within a subduction interface mélange. *Earth Planet. Sci. Lett.* **488**, 27–35 (2018).
89. Taylor, F. et al. Rupture across arc segment and plate boundaries in the 1 April 2007 Solomons earthquake. *Nat. Geosci.* **1**, 253–257 (2008).
90. Carvajal, M., Cisternas, M. & Catalān, P. A. Source of the 1730 Chilean earthquake from historical records: implications for the future tsunami hazard on the coast of metropolitan Chile. *J. Geophys. Res. Solid Earth* **122**, 3648–3660 (2017).
91. Contreras-Reyes, E. & Carrizo, D. Control of high oceanic features and subduction channel on earthquake ruptures along the Chile–Peru subduction zone. *Phys. Earth Planet. Inter.* **186**, 49–58 (2011).
92. Song, T. & Simons, M. Large trench-parallel gravity variations predict seismogenic behavior in subduction zones. *Science* **301**, 630–633 (2003).
93. Wells, R. E., Blakely, R. J., Sugiyama, Y., Scholl, D. W. & Dinterman, P. A. Basin-centered asperities in great subduction zone earthquakes: a link between slip, subsidence, and subduction erosion? *J. Geophys. Res. Solid Earth* **108**, 2507 (2003).
94. Bassett, D., Sandwell, D. T., Fialko, Y. & Watts, A. B. Upper-plate controls on co-seismic slip in the 2011 magnitude 9.0 Tohoku-Oki earthquake. *Nature* **531**, 92–96 (2016).
95. Wells, R., Weaver, C. & Blakely, R. Fore-arc migration in Cascadia and its neotectonic significance. *Geology* **26**, 759–762 (1998).
96. Melnick, D., Bookhagen, B., Strecker, M. R. & Echtler, H. P. Segmentation of megathrust rupture zones from fore-arc deformation patterns over hundreds to millions of years, Arauco peninsula, Chile. *J. Geophys. Res. Solid Earth* **114**, B01407 (2009).
97. McCaffrey, R. The tectonic framework of the Sumatran subduction zone. *Annu. Rev. Earth Planet. Sci.* **37**, 345–366 (2009).
98. Uyeda, S. & Kanamori, H. Back-arc opening and the mode of subduction. *J. Geophys. Res. Solid Earth* **84**, 1049–1061 (1979).
99. Scholz, C. & Campos, J. On the mechanism of seismic decoupling and back arc spreading at subduction zones. *J. Geophys. Res. Solid Earth* **100**, 22103–22115 (1995).
100. Heuret, A. & Lallemand, S. Plate motions, slab dynamics and back-arc deformation. *Phys. Earth Planet. Inter.* **149**, 31–51 (2005).
101. Wallace, L., Fagereng, Å. & Ellis, S. Upper plate tectonic stress state may influence interseismic coupling on subduction megathrusts. *Geology* **40**, 895–898 (2012).
102. Heuret, A., Conrad, C., Funiciello, F., Lallemand, S. & Sandri, L. Relation between subduction megathrust earthquakes, trench sediment thickness and upper plate strain. *Geophy. Res. Lett.* **39**, L05304 (2012).
103. Fagerang, Å. & Ellis, S. On factors controlling the depth of interseismic coupling on the Hikurangi subduction interface, New Zealand. *Earth Planet. Sci. Lett.* **278**, 120–130 (2009).
104. Shapiro, N. M., Ritzwoller, M. H. & Engdahl, E. R. Structural context of the great Sumatra–Andaman Islands earthquake. *Geophys. Res. Lett.* **35**, L05301 (2008).
105. Clift, P. & Vannucchi, P. Controls on tectonic accretion versus erosion in subduction zones: implications for the origin and recycling of the continental crust. *Rev. Geophys.* **42**, RG2001 (2004).
106. Storch, I., Buske, S., Victor, P. & Oncken, O. Seismic images of the northern Chilean subduction zone at 19° 40′ S, prior to the 2014 Iquique earthquake. *Geophys. J. Int.* **225**, 1048–1061 (2021).
107. Park, J., Tsuru, T., Kodaira, S., Cummins, P. & Kaneda, Y. Splay fault branching along the Nankai subduction zone. *Science* **297**, 157–1160 (2002).
108. Tsuji, T. et al. Extension of continental crust by anelastic deformation during the 2011 Tohoku-Oki earthquake: the role of extensional faulting in the generation of a great tsunami. *Earth Planet. Sci. Lett.* **364**, 44–58 (2013).
109. Plafker, G. Tectonic deformation associated with the 1964 Alaska earthquake: the earthquake of 27 March 1964 resulted in observable crustal deformation of unprecedented areal extent. *Science* **48**, 1675–1687 (1965).
110. Farías, M., Comte, D., Roecker, S., Carrizo, D. & Pardo, M. Crustal extensional faulting triggered by the 2010 Chilean earthquake: the Pichilemu seismic sequence. *Tectonics* **30**, TC6010 (2011).
111. Ashford, S. A., Boulanger, R. W., Donahue, J. L. & Stewart, J. P. *Geotechnical Quick Report on the Kanto Plain Region During the March 11, 2011, off Pacific Coast of Tohoku Earthquake, Japan* (GEER, 2011).
112. Serey, A. et al. Landslides induced by the 2010 Chile megathrust earthquake: a comprehensive inventory and correlations with geological and seismic factors. *Landslides* **16**, 1153–1165 (2019).
113. Douglas, J. & Edwards, B. Recent and future developments in earthquake ground motion estimation. *Earth Sci. Rev.* **160**, 203–219 (2016).
114. Oth, A., Miyake, H. & Bindi, D. On the relation of earthquake stress drop and ground motion variability. *J. Geophys. Res. Solid Earth* **122**, 5474–5492 (2017).
115. Wirth, E., Frankel, A., Marafi, N., Vidale, J. & Stephenson, W. Broadband synthetic seismograms for magnitude 9 earthquakes on the Cascadia megathrust based on 3D simulations and stochastic synthetics, Part 2: rupture parameters and variability. *Bull. Seismol. Soc. Am.* **108**, 2370–2388 (2018).
116. Somerville, P., Smith, N., Graves, R. & Abrahamson, N. Modification of empirical strong ground motion attenuation relations to include the amplitude and duration effects of rupture directivity. *Seismol. Res. Lett.* **68**, 199–222 (1997).
117. Chandramohan, R., Baker, J. & Deierlein, G. Quantifying the influence of ground motion duration on structural collapse capacity using spectrally equivalent records. *Earthq. Spectra* **32**, 927–950 (2016).
118. McGuire, J., Zhao, L. & Jordan, T. Predominance of unilateral rupture for a global catalog of large earthquakes. *Bull. Seismol. Soc. Am.* **92**, 3309–3317 (2002).
119. Mai, P., Spudich, P. & Boatwright, J. Hypocenter locations in finite-source rupture models. *Bull. Seismol. Soc. Am.* **95**, 965–980 (2005).
120. Melgar, D. & Hayes, G. The correlation lengths and hypocentral positions of great earthquakes. *Bull. Seismol. Soc. Am.* **109**, 2582–2593 (2019).
121. Ishii, M., Shearer, P., Houston, H. & Vidale, J. Extent, duration and speed of the 2004 Sumatra–Andaman earthquake imaged by the Hi-Net array. *Nature* **435**, 933–936 (2005).
122. Baltay, A. S., Hanks, T. C. & Beroza, G. C. Stable stress-drop measurements and their variability: implications for ground-motion prediction. *Bull. Seismol. Soc. Am.* **103**, 211–222 (2013).
123. Cotton, F., Archuleta, R. & Causse, M. What is sigma of the stress drop? *Seismol.Res. Lett.* **84**, 42–48 (2013).
124. Allmann, B. P. & Shearer, P. M. Global variations of stress drop for moderate to large earthquakes. *J. Geophys. Res. Solid Earth* **114**, B01310 (2009).
125. Denolle, M. & Shearer, P. New perspectives on self-similarity for shallow thrust earthquakes. *J. Geophys. Res. Solid Earth* **121**, 6533–6565 (2016).
126. Uchide, T., Shearer, P. & Imanishi, K. Stress drop variations among small earthquakes before the 2011 Tohoku-Oki, Japan, earthquake and implications for the main shock. *J. Geophys. Res. Solid Earth* **119**, 7164–7174 (2014).
127. Uchida, N. & Bürgmann, R. Repeating earthquakes. *Annu. Rev. Earth Planet. Sci.* **47**, 305–332 (2019).
128. Wirth, E. & Frankel, A. Impact of down-dip rupture limit and high-stress drop subevents on coseismic land-level change during cascadia megathrust earthquakes. *Bull. Seismol. Soc. Am.* **109**, 2187–2197 (2019).
129. Das, S. The need to study speed. *Science* **317**, 905–906 (2007).
130. Wang, D., Mori, J. & Koketsu, K. Fast rupture propagation for large strike-slip earthquakes. *Earth Planet. Sci. Lett.* **40**, 115–126 (2016).
131. Ye, L., Lay, T., Kanamori, H. & Rivera, L. Rupture characteristics of major and great (Mw ≥ 7.0) megathrust earthquakes from 1990 to 2015: 1. Source parameter scaling relationships. *J. Geophys. Res. Solid Earth* **121**, 826–844 (2016).
132. Ammon, C. J. et al. Rupture process of the 2004 Sumatra–Andaman earthquake. *Science* **308**, 1133–1139 (2005).
133. Delouis, B., Nocquet, J. & Vallée, M. Slip distribution of the February 27, 2010 Mw=8.8 Maule earthquake, central Chile, from static and high-rate GPS, InSAR, and broadband teleseismic data. *Geophys. Res. Lett.* **37**, L17305 (2010).
134. Lay, T. et al. Teleseismic inversion for rupture process of the 27 February 2010 Chile (Mw 8.8) earthquake. *Geophys. Res. Lett.* **37**, L13301 (2010).
135. Koper, K. D., Hutko, A. R. & Lay, T. Along-dip variation of teleseismic short-period radiation from the 11 March 2011 Tohoku earthquake (Mw 9.0). *Geophys. Res. Lett.* **38**, L21309 (2011).
136. Yue, H. & Lay, T. Inversion of high rate (1 sps) GPS data for rupture process of the 11 March 2011 Tohoku earthquake (Mw 9.1). *Geophys. Res. Lett.* **38**, L00G09 (2011).
137. Das, S. in *Perspectives on European Earthquake Engineering and Seismology* (ed. Ansal, A.) 1–20 (Springer, 2015).
138. Bruhat, L., Fang, Z. & Dunham, E. Rupture complexity and the supershear transition on rough faults. *J. Geophys. Res. Solid Earth* **121**, 210–224 (2016).
139. Hyndman, R. D. Downdip landward limit of Cascadia great earthquake rupture. *J. Geophys. Res. Solid. Earth* **118**, 5530–5549 (2013).
140. Heuret, A., Lallemand, S., Funiciello, F., Piromallo, C. & Faccenna, C. Physical characteristics of subduction interface type seismogenic zones revisited. *Geochem. Geophys. Geosystems* **12**, Q01004 (2011).
141. Garrett, E. et al. A systematic review of geological evidence for Holocene earthquakes and tsunamis along the Nankai–Suruga Trough, Japan. *Earth Sci. Rev.* **159**, 337–357 (2016).
142. Clark, K. et al. Geological evidence for past large earthquakes and tsunamis along the Hikurangi subduction margin, New Zealand. *Mar. Geol.* **412**, 39–172 (2019).
143. Moernaut, J. Time-dependent recurrence of strong earthquake shaking near plate boundaries: a lake sediment perspective. *Earth Sci. Rev.* **210**, 103344 (2020).
144. Walton, M. et al. Toward an integrative geological and geophysical view of cascadia subduction zone earthquakes. *Annu. Rev. Earth Planet. Sci.* **49**, 367–398 (2021).
145. Goldfinger, C., Ikeda, Y., Yeats, R. & Ren, J. Superquakes and supercycles. *Seismol. Res. Lett.* **84**, 24–32 (2013).
146. Barbot, S. Frictional and structural controls of seismic super-cycles at the Japan Trench. *Earth Planets Space* **72**, 1–25 (2020).
147. Rosenau, M., Corbi, F. & Dominguez, S. Analogue earthquakes and seismic cycles: experimental modelling across timescales. *Solid Earth* **8**, 597–635 (2017).
148. Salditch, L. et al. Earthquake supercycles and long-term fault memory. *Tectonophysics* **774**, 228289 (2020).
149. Howarth, J. et al. Calibrating the marine turbidite palaeoseismometer using the 2016 Kaikōura earthquake. *Nat. Geosci.* **14**, 161–167 (2021).
150. Struble, W. et al. The preservation of climate driven landslide dams in western oregon. *J. Geophys. Res. Earth Surf.* **126**, e2020JF005908 (2021).
151. Nanayama, F. et al. Unusually large earthquakes inferred from tsunami deposits along the Kuril trench. *Nature* **424**, 660–663 (2003).
152. Satake, K. Mechanism of the 1992 Nicaragua tsunami earthquake. *Geophys. Res. Lett.* **21**, 2519–2522 (1994).
153. Satake, K., Fujii, Y., Harada, T. & Namegaya, Y. Time and space distribution of coseismic slip of the 2011 Tohoku earthquake as inferred from tsunami waveform data. *Bull. Seismol. Soc. Am.* **103**, 1473–1492 (2013).
154. Melgar, D. & Bock, Y. Near-field tsunami models with rapid earthquake source inversions from land- and ocean-based observations: the potential for forecast and warning. *J. Geophys. Res. Solid Earth* **118**, 5939–5955 (2013).

155. Lotto, G., Nava, G. & Dunham, E. Should tsunami simulations include a nonzero initial horizontal velocity? *Earth Planets Space* **69**, 1–14 (2017).
156. Tappin, D. T. et al. Did a submarine landslide contribute to the 2011 Tohoku tsunami? *Mar. Geol.* **357**, 344–361 (2014).
157. Melgar, D., Williamson, A. & Salazar-Monroy, E. Differences between heterogenous and homogenous slip in regional tsunami hazards modelling. *Geophys. J. Int.* **219**, 553–562 (2019).
158. Moore, G. et al. Three-dimensional splay fault geometry and implications for tsunami generation. *Science* **318**, 1128–1131 (2007).
159. Wendt, J., Oglesby, D. L. & Geist, E. L. Tsunamis and splay fault dynamics. *Geophys. Res. Lett.* **36**, L15303 (2009).
160. Baba, T., Cummins, P. R., Hori, T. & Kaneda, Y. High precision slip distribution of the 1944 Tonankai earthquake inferred from tsunami waveforms: possible slip on a splay fault. *Tectonophysics* **426**, 119–134 (2006).
161. Fan, W., Bassett, D., Jiang, J., Shearer, P. & Ji, C. Rupture evolution of the 2006 Java tsunami earthquake and the possible role of splay faults. *Tectonophysics* **721**, 143–150 (2017).
162. Liberty, L., Brothers, D. & Haeussler, P. Tsunamigenic splay faults imply a long-term asperity in southern Prince William Sound, Alaska. *Geophys. Res. Lett.* **46**, 3764–3772 (2019).
163. Bell, R., Holden, C., Power, W., Wang, X. & Downes, G. Hikurangi margin tsunami earthquake generated by slow seismic rupture over a subducted seamount. *Earth Planet. Sci. Lett.* **397**, 1–9 (2014).
164. Riquelme, S., Schwarze, H., Fuentes, M. & Campos, J. Near-field effects of earthquake rupture velocity into tsunami runup heights. *J. Geophys. Res. Solid Earth* **125**, e2019JB018946 (2020).
165. Williamson, A., Melgar, D. & Rim, D. The effect of earthquake kinematics on tsunami propagation. *J. Geophys. Res. Solid Earth* **124**, 11639–11650 (2019).
166. Ma, S. & Hirakawa, E. Dynamic wedge failure reveals anomalous energy radiation of shallow subduction earthquakes. *Earth Planet. Sci. Lett.* **375**, 113–122 (2013).
167. Okada, Y. Surface deformation due to shear and tensile faults in a half-space. *Bull. Seismol. Soc. Am.* **75**, 1135–1154 (1985).
168. Lindsey, E. et al. 2021. Slip rate deficit and earthquake potential on shallow megathrusts. *Nat. Geosci.* **14**, 321–326 (2021).
169. Materna, K., Bartlow, N., Wech, A., Williams, C. & Bürgmann, R. Dynamically triggered changes of plate interface coupling in southern Cascadia. *Geophys. Res. Lett.* **46**, 12890–12899 (2019).
170. Goldfinger, C. et al. *Turbidite Event History — Methods and Implications for Holocene Paleoseismicity of the Cascadia Subduction Zone (No. 1661-F)* (US Geological Survey, 2012).
171. Pearl, J., Black, B., Pringle, P., Sherrod, B. & Angster, S. Multiproxy dendrochronological dating of coseismic land-level changes in the Puget lowlands [abstract EP035-01] (American Geophysical Union, 2020).
172. van Daele, M. et al. Distinguishing intraplate from megathrust earthquakes using lacustrine turbidites. *Geology* **47**, 127–130 (2019).
173. Erickson, B. et al. The community code verification exercise for simulating sequences of earthquakes and aseismic slip (SEAS). *Seismol. Res. Lett.* **91**, 874–890 (2020).
174. Brown, J., Prejean, S., Beroza, G., Gomberg, J. & Haeussler, P. Deep low-frequency earthquakes in tectonic tremor along the Alaska–Aleutian subduction zone. *J. Geophys. Res. Solid Earth* **118**, 1079–1090 (2013).
175. Collot, J. et al. Are rupture zone limits of great subduction earthquakes controlled by upper plate structures? Evidence from multichannel seismic reflection data acquired across the northern Ecuador–southwest Colombia margin. *J. Geophys. Res. Solid Earth* **109**, B11103 (2004).
176. Haeussler, P. & Plafker, G. *Earthquakes in Alaska: Open-File Report 95-624* (US Geological Survey, 2004).
177. Hayes, G. The finite, kinematic rupture properties of great-sized earthquakes since 1990. *Earth Planet. Sci. Lett.* **468**, 94–100 (2017).
178. Hong, I. et al. A 600-year-long stratigraphic record of tsunamis in south-central Chile. *Holocene* **27**, 39–51 (2017).
179. Lay, T. et al. The 2006–2007 Kuril Islands great earthquake sequence. *J. Geophys. Res. Solid Earth* **114**, B11308 (2009).
180. Moernaut, J. et al. Larger earthquakes recur more periodically: new insights in the megathrust earthquake cycle from lacustrine turbidite records in south-central Chile. *Earth Planet. Sci. Lett.* **481**, 9–19 (2018).
181. Mondal, D. et al. Microatolls document the 1762 and prior earthquakes along the southeast coast of Bangladesh. *Tectonophysics* **745**, 196–213 (2018).
182. Okal, E., Borrero, J. & Synolakis, C. Evaluation of tsunami risk from regional earthquakes at Pisco, Peru. *Bull. Seismol. Soc. Am.* **96**, 634–1648 (2006).
183. Gripp, A. & Gordon, R. Young tracks of hotspots and current plate velocities. *Geophys. J. Int.* **150**, 321–361 (2002).
184. Christophersen, A., Berryman,K. & Litchfield, N. *The GEM Faulted Earth Project* (GEM, 2015); https://www.globalquakemodel.org/gempublications/The-GEM-Faulted-Earth-Project.
185. Hayes, G. et al. Slab2, a comprehensive subduction zone geometry model. *Science* **362**, 58–61 (2018).
186. Ho, T., Satake, K., Watada, S. & Fujii, Y. Source estimate for the 1960 Chile earthquake from joint inversion of geodetic and transoceanic tsunami data. *J. Geophys. Res. Solid Earth* **124**, 2812–2828 (2019).
187. Ichinose, G., Somerville, P., Thio, H., Graves, R. & O'Connell, D. Rupture process of the 1964 Prince William Sound, Alaska, earthquake from the combined inversion of seismic, tsunami, and geodetic data. *J. Geophys. Res. Solid Earth* **112**, B07306 (2007).
188. Atwater, B. F. et al. *The Orphan Tsunami of 1700: Japanese Clues to a Parent Earthquake in North America (No. 1707)* (US Geological Survey, 2005).
189. Satake, K., Wang, K. & Atwater, B. F. Fault slip and seismic moment of the 1700 Cascadia earthquake inferred from Japanese tsunami descriptions. *J. Geophys. Res. Solid Earth* **108**, 2535 (2003).
190. Skarlatoudis, A., Somerville, P. & Thio, H. Source-scaling relations of interface subduction earthquakes for strong ground motion and tsunami simulation. *Bull. Seismol. Soc. Am.* **106**, 1652–1662 (2016).
191. Allen, T. & Hayes, G. Alternative rupture-scaling relationships for subduction interface and other offshore environments. *Bull. Seismol. Soc. Am.* **107**, 1240–1253 (2017).

Acknowledgements
The authors thank G. Hayes and J. Gomberg for helpful and constructive feedback, which helped to improve this manuscript. V.J.S. was supported, in part, by NASA ROSES grant 80NSSC21K0841. D.M. was supported by the Millennium Scientific Initiative (ICM) of the Chilean government through grant NC160025 'Millennium Nucleus CYCLO The Seismic cycle along subduction zones', FONDECYT grants 1181479 and 1190258, and the ANID PIA Anillo ACT192169.

Author contributions
E.A.W. and V.J.S. co-led the writing of the manuscript and contributed equally to this article. All authors contributed to the research, writing, figure preparation and editing of this Review.

Competing interests
The authors declare no competing interests.

Peer review information
Nature Reviews Earth & Environment thanks K. Satake, S. Lallemand and the other, anonymous, reviewer(s) for their contribution to the peer review of this work.

Publisher's note
Springer Nature remains neutral with regard to jurisdictional claims in published maps and institutional affiliations.

Supplementary information
The online version contains supplementary material available at https://doi.org/10.1038/s43017-021-00245-w.